Feasibility study of novel seasonal energy storage technologies for residential systems

Francesca Corvaglia

Master of Science Thesis

Picture © https://neosun.com/

TU Delft

Faculty of Mechanical, Maritime and Materials Engineering

Feasibility study of novel seasonal energy storage technologies for residential systems

by

Francesca Corvaglia

MASTER OF SCIENCE THESIS

to obtain the degree of Master of Science in
Mechanical Engineering - Energy and Process Technology
at the Delft University of Technology

November 19th, 2021

Student number:	5032822	
Supervisors:	Dr. R. Kortlever	Department of Process & Energy, 3mE, TU Delft
	Dr.ir. G. R. Chandra Mouli	Department of Electrical Sustainable Energy, EECMS, TU Delft
	Dr.ir. N. van der Blij	Department of Electrical Sustainable Energy, EECMS, TU Delft

TU Delft Delft University of Technology

Preface

This report concludes nine months of engaging work on this project, and two intense years of study at TU Delft. With this thesis, I hope to draw some attention to alternative solutions that could become an important part of the road towards the decarbonization of the energy sector in the near future.

Working at this project in this particular times was not easy, therefore I am even more grateful to all the people who helped me through this journey. Thank you to my supervisors Ruud Kortlever and Gautham Chandra Mouli for their kind words and the constant support they gave me, even through a screen. Thank you to Nils van der Blij, who first gave me the idea for the project and supervised the first delicate months of work. Thank you also to Ibrahim Diab and Wiljan Vermeer for their precious help.

Abstract

The growing global energy demand and correlated rise in carbon emissions is forcing us to increase the use of renewable sources. The residential sector represents a large part of the total energy consumption, and European governments are investing in distributed PV to increase the renewable share in this sector. However, on top of the solar power variability, residential systems are also characterized by very unstable load profiles. This issue can be solved by incorporating energy storage, that has many technical and economic benefits for the prosumer, especially if a long-term seasonal storage technology is used. Among all the available storage types, after an extensive literature study, some developing technologies proved to be suitable for this purpose: redox flow batteries (all-vanadium, hydrogen-bromide, zinc-bromide) and hydrogen systems.

For this work, a model was built in MATLAB Simulink to study and reproduce the behaviour of these storage systems in a grid-connected residential environment, and an optimization was set up to find the optimal sizing of the components and investigate the economic feasibility of the whole system. The models results proved that in the present scenario, storage integration is still too expensive with these technologies. However, future projections with different incentive scenarios demonstrate the potential of vanadium and zinc-bromine batteries, and highlight a dramatic cost reduction for hydrogen systems.

Contents

List of Abbreviations

AEL Alkaline Electrolyser

AFC Alkaline Fuel Cell

BOP Balance of Power

CAES Compressed Air Energy Storage

COP Coefficient of Performance

DSO Distribution System Operator

ESS Energy Storage System(s)

HBFB Hydrogen-Bromine Redox Flow Battery

HHV Higher Heating Value

LCOE Levelized Cost Of Energy

PCS Power Conversion System

PEMEL Polymer Electrolyte Membrane Electrolyser

PEMFC Polymer Electrolyte Membrane Fuel Cell

PHS Pumped Hydro Storage

PV Photovoltaic

RES Renewable Energy Source(s)

RFB Redox Flow Battery

SC Self-consumption

SHE Standard Hydrogen Electrode

SOEL Solid Oxide Electrolyser

SOFC Solid Oxide Fuel Cell

TD Transmission & Distribution

VRFB Vanadium Redox Flow Battery

ZBFB Zinc-Bromine Redox Flow Battery

cSi Crystalline Silicon

List of Symbols

Symbols (in order of appaerance)

P	Power	W
η	PV panels efficiency (PV) - Overpotential (electrochemical)	% - V
G	Solar irradiance	W/m^2
T	Temperature	°C/K
A	PV panel area	m^2
α	Temperature coefficient	°C^{-1}
v	Velocity	m/s
V	Voltage	V
ΔG	Change in Gibb's free energy	J
n	Number of exchanged electrons	-
F	Faraday's constant	C/mol
R	Ideal gas constant - Resistance	J/K*mol - Ω
a	Activity	-
I	Current	A
N	Number of storage cells	-
C	Electrolyte concentration	M
Vol	Electrolyte volume	L
Q	Electrolyte flow rate	L/s
t	Time	s
i	Current density	A/cm^2
E	Energy	J
ϵ	Storage energy efficiency	%
LCOE	Levelized cost of electricity	€/kWh
$Cost$	Cost (general)	€
In	Investment cost	€
Op	Operation & maintenance cost	€/year
D	Compound interest factor	-
SOC	Storage state of charge	%
SC	Self-consumption level	%

Subscripts (in order of appaerance)

M	Relative to PV module
cell	Relative to storage cell
OCV	Open circuit voltage
an	Relative to anode
cat	Relative to cathode
c	Relative to charge (stored by the storage system)
d	Relative to discharge (delivered by the storage system)

PV	Photovoltaic
S	Storage
S,c	Storage charge (stored by the storage system)
S,d	Storage discharge (delivered by the storage system)
G	Grid
G,i	Grid in (bought from the grid)
G,o	Grid out (sold to the grid)
L	Load
P,L	From photovoltaic to load

1 Introduction

1.1. Energy transition

Global demand for energy continues to rise, led by an expanding economy, population growth, stronger heating and cooling needs and growing urbanization [1]. The increased usage of fossil fuels significantly contributes to an increase in the atmospheric CO_2 concentration [2] which negatively impacts the climate, and is compelling governments to seek more sustainable options to meet the rising energy demand. In 2019 the European Commission proposed the European Green Deal, an action plan that aims at making the European Union climate neutral in 2050 [3].

As a result of governments policies, the world is experiencing unprecedented growth in renewable energy deployment. It is estimated that in the European Union, renewable energy sources (RES) will account for 80% of new capacity in 2040, wind power will become the leading source of electricity due to strong growth both onshore and offshore, and millions of households, communities and businesses will invest directly in distributed solar PV [4]. However, the increased share of variable RES (solar and wind power) is a challenge for energy systems, as it leads to unreliability and instability of the electricity supply due to the mismatch between output power from RES and power demanded from the load.

While wind power is mainly used for large scale energy production, due to its high investment and maintenance costs, space requirements and noisy operation [5], the growth potential of distributed PV for households is particularly high, due to lowered investments costs and incentives [6]. Nowadays, the residential sector is responsible for almost 30% of the total electricity consumption [7]. Residential systems are also characterized by very unstable load profiles, deriving from variable usage of appliances and heating or cooling during the day or between seasons. A way to cope with this is by incorporating energy storage.

1.2. Energy storage

Energy storage allows energy to be accumulated during high renewable generation or low demand periods, and to be used during low renewable production or high demand periods. Storage devices in combination with PV power can be used for

electricity procurement in remote locations (stand-alone systems) or, if connected to the grid, they can provide several benefits for all the actors involved. Depending on their type, energy storage systems (ESS) are useful for energy management, peak shaving, load leveling, seasonal storage, frequency regulation and backup power [8]. In order to determine which technologies are most suitable for small scale systems, an overview of their benefits and requirements for storage integration to the grid is presented.

1.2.1. Grid-connected storage benefits

The electrical grid is a critical component of the energy infrastructure that connects point of use and power generation. Distributed generation with variable RES has introduced bidirectional power flows in the electricity network, where consumers have the potential to feed power to the grid (becoming *prosumers*), but at the same time experience instability and unreliability of their own power supply [9]. The technical and economical benefits of integrating energy storage in residential systems with distributed PV have been reviewed in recent papers [9–12]:

Costs reduction is manifested in both initial investment and periodic electric bill costs. Energy storage allows to maximize self-consumption of solar power, to take advantage of time of use tariffs, and to optimize the capacity (hence price) of the installed system, as energy demand peaks can be shared between PV and storage [9]. Moreover, residential PV-storage system installation could give access to the incentives and feed-in tariffs that many governments are funding to promote RES integration.

Benefits for behind-the-meter systems mainly come from the time shifting ability of storage technologies. Using energy stored during irradiation peaks, the ESS is able to reduce demand highs and lows (peak shaving) and minimize fluctuations of the load (load leveling) as shown in Figure 1.1. Moreover, in case of a power interruption or surge from the main grid, uninterruptible power supply (UPS) or backup power can be provided by the ESS.

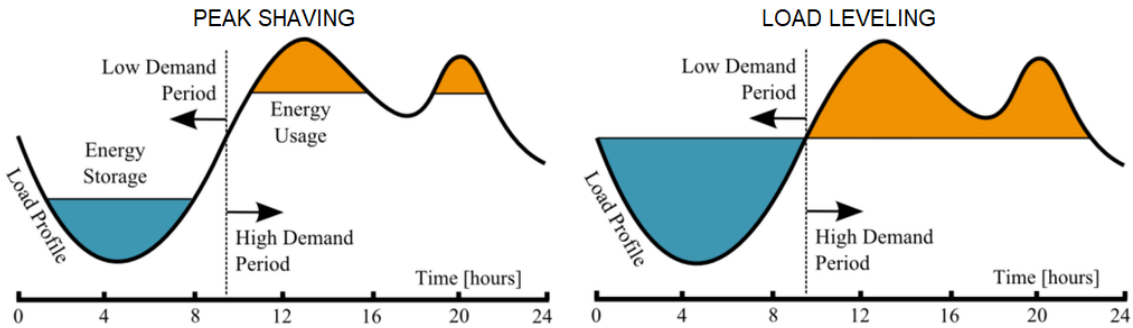

Figure 1.1: Representation of the peak shaving and load leveling action of an energy storage system [13]

Energy trade can be performed by the owner of a PV-storage independent system, taking advantage of the fluctuating price of electricity. Furthermore, through the Energy Management System connected to the local controller of the PV-storage system, the owner can actively check and manage his own power consumption.

Ancillary services & Grid support can be provided by the ESS, like keeping frequency and voltage within the stability limits, reducing congestion during high demand periods or delaying costly investment in transport & development required in case of load growth.

Application family	Application
Costs reduction	Self consumption increase System capacity sizing optimization Access to incentives/feed-in tariffs Time of use tariffs exploitation
Behind-the-meter benefits	Peak shaving Load leveling Seasonal storage Uninterruptible power supply (UPS) Backup power
Energy trade	Independence from electricity market prices Arbitrage in electricity trade Management of own energy consumption
Ancillary services & Grid support	Frequency regulation Voltage support TD investment deferral Congestion relief

Table 1.1: Benefits of energy storage technologies for residential systems [8–10, 14]

1.2.2. Grid-connected storage requirements

To narrow the range of options and find the ESS with higher potential for a residential grid-connected application, several factors can be taken into consideration:

Discharge times
Grid applications are generally divided into three categories:

- Energy management, that requires long discharge times (days to months)
- Time shifting, that requires discharge times of minutes-hours

- Power quality, that requires fast response and short discharge times (seconds)

To effectively improve PV integration and reduce grid dependency throughout the whole year, energy management and time shifting applications are essential, therefore the most suitable type of technologies are long-term (or long-duration) storage systems, characterized by high energy capacity, modest power rating and long discharge times (> 8 hours) [15]. Moreover, from the prosumer point of view larger benefits come from this application, as they directly reduce the electricity bills and increase the reliability of the energy system. Therefore, only long-duration storage technologies are preferred for this analysis.

Rated power
A small-scale ES system should be able to store as much solar power as possible and minimize intake from the main grid, covering generation drops and load peaks. In order to capture all the solar power produced, a microgrid ESS comprising some houses is estimated to need approximately 50 kW [15] of power. A storage technology that, with one or few devices in parallel, is able to reach this threshold it preferred.

Lifetime and cycle life
Ideally, a cost-effective ESS should have a similar lifetime as the associated energy source. Rooftop PV panels have an approximate lifetime of 20 years, that assuming one full charge-discharge cycle per day, correspond to 7300 cycles. A suitable ESS should preferably meet these lifetime and cycle life requirements.

Environment compatibility
Safety is a major concern in residential areas: toxic and polluting materials must be avoided. Other features like low maintenance requirements and low noise levels are appreciated. Size and land occupancy are not too limited but have boundaries. For example, large mechanical storage methods like pumped hydro (PHS) and compressed air (CAES) require huge spaces and proximity of specific environments (respectively water reservoirs at different heights and natural underground caverns near a gas turbine plant). The site-dependency of these technologies makes them difficult to be integrated in a residential environment.

1.3. Available storage technologies

Energy storage technologies are generally classified in 5 types, according to the technology used and form of stored energy, as shown in Figure 1.2: mechanical, electrochemical (electrochemical batteries and redox flow batteries), electrical, chemical, thermal.

Requirements for ESS are widely varying and no single technology is able to meet all of them, but each one may offer certain attributes and merits for a certain application. Several review papers [8, 13, 14, 16–20] have classified existing ESS in

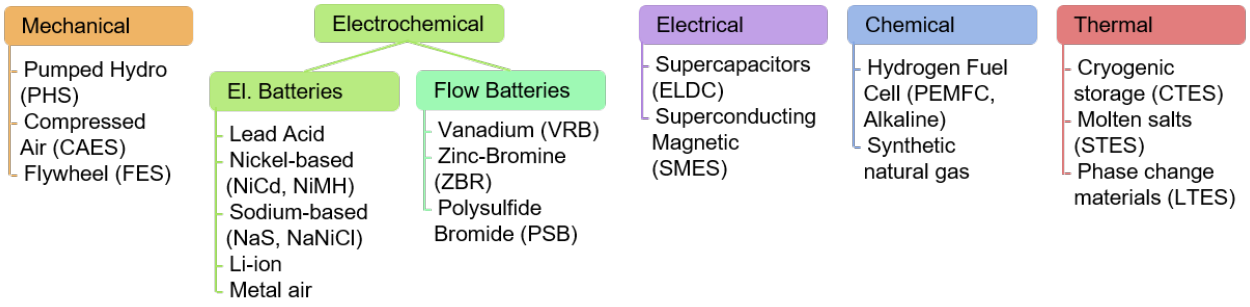

Figure 1.2: Classification of energy storage technologies [8]

order to determine which application(s) they could satisfy.

As mentioned above, for the sake of this study only long-duration energy storage technologies with discharge duration greater than 8 hours will be considered.

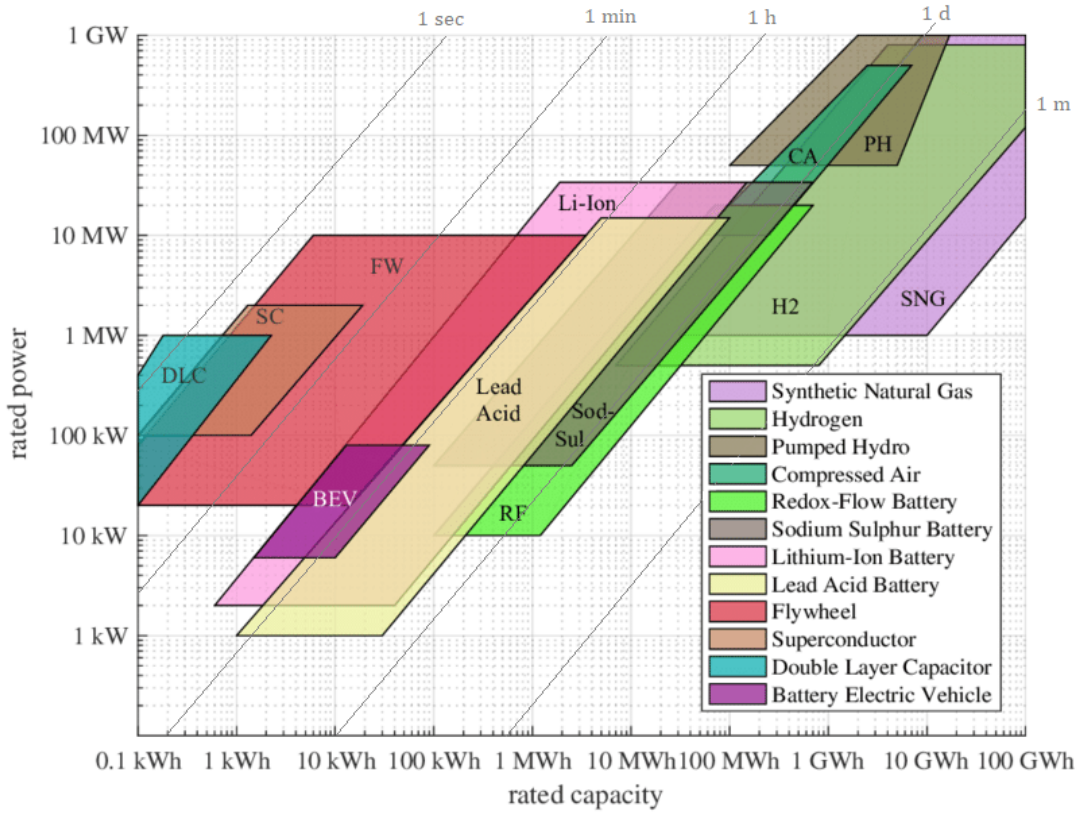

Figure 1.3: Ragone plot of energy storage technologies [21]

From the Ragone plot showed in Figure 1.3, it is already possible to to identify the long-duration storage technologies:

- Lead-acid (LA), nickel based (BEV), sodium based (NaS) and Li-ion electrochemical batteries

- Redox flow batteries (B)
- Hydrogen (H_2) and syngas (SNG) chemical fuel storage
- Pumped hydro (PHS) and compressed air (CAES) mechanical storage

The same storage types are identified as the most suitable for seasonal storage and time shifting purposes by other review studies [8, 13]. In the following part, a short description of each of these technologies is given, focusing on possible application to small scale systems.

1.3.1. Electrochemical batteries

Electrochemical batteries are the most popular and mature energy storage devices [18]. They store energy by creating charged ions through chemical reactions between two charged plates (electrodes). During charging, electricity is used to induce electrochemical reactions to create ions, while during discharging these ions are recombined and chemical energy is converted back to electricity as flow of electrons in DC form [19]. Existing types of batteries employ a diverse range of materials and show different features:

- *Lead-acid batteries* are used in vehicles and stationary applications. They are low cost, relatively efficient and reliable, however they have low energy density and specific power, limited cycle life, high maintenance costs, environmental impact and suffer degradation for deep discharge [8, 14, 20, 22].
- *Nickel-based batteries* perform well at low temperatures, have high energy density and long cycle life, but lower energy efficiency. The most commercialized is the NiCd battery, which however suffers from memory effects and uses harmful chemicals [8, 22–24] (banned for consumers in EU since 2006 [14]). A similar but less harmful alternative are NiMH batteries, which have similar application as Li-ion ones [14].
- *Sodium-based batteries* require high temperatures (270-350°C) to work. NaS ones are considered a promising solution for stationary EES, due to their high energy and power density, low maintenance needs, long cycle life and the use of inexpensive and non-toxic materials. However, they show high initial costs and some safety problems [8, 20, 25]. NaNiCl or ZEBRA (Zero Emission Battery Research) batteries have better safety and maintenance characteristics but poorer energy and power density, and have been employed in EV designs [8, 14, 20, 24].
- *Lithium-ion batteries* are the most important storage technology, especially in portable and mobile applications, due to their high cell voltage (3.7 V) and efficiency (>95%). They are very versatile, thanks to the wide range of discharge times, but have serious safety risks [16, 26, 27]. They are currently quite expensive, but it is expected that their price will drop in the future [28].

- *Metal-air batteries* are a new, promising and still developing technology, as they could be the most compact and least expensive environmentally benign battery. They are composed of an anode made from pure metal and a cathode connected to a supply of air, from which oxygen is used in the reaction. Currently only Zn-air batteries have been tested and show hybrid properties between fuel cells and conventional batteries, however electrical recharging is still difficult and inefficient [16, 20, 24].

1.3.2. Redox flow batteries

In redox flow batteries (RFB), energy is accumulated in two liquid electrolyte solutions, stored in separate tanks. During charging or discharging, the solutions are pumped to electrochemical cells, where redox reactions occur across selective membranes, transforming electricity into chemical potential or vice versa. The main advantage of RFB is their ability to decouple their power section from their energy section: this determines ease of scalability, no self-discharge, no degradation for deep discharge and low maintenance needs. These features make RFB a very attractive technology for RES integration storage. However, they have lower efficiencies compared to some electrochemical batteries, and high investment cost [29, 30]. The main types employ materials like vanadium (VRFB), zinc-bromine (ZBFB) and polysulfide bromide (PSB). Organic RFB are also being studied as an environmental friendly and inexpensive alternative, however they have not yet shown competitive performance [31].

1.3.3. Power to chemicals

Energy contained in chemical bonds of fuels is much denser than energy stored in electrochemical batteries. Fuels like hydrogen and synthetic natural gas (methane) can be produced using excess renewable electricity and stored for later use. Among those, pure hydrogen has the highest gravimetric energy density (142 MJ/kg HHV) but its conversion to other chemical compounds (ex. CH_4) facilitates its storage [16, 24].

- *Hydrogen* produced from water electrolysis is the most environmentally friendly energy carrier. A typical hydrogen storage system consists of an electrolyser, a hydrogen storage tank and a fuel cell, which can be of three main types: alkaline, PEMFC or SOFC [14, 16]. "Unitized" regenerative fuel cells, where synthesis and oxidation occur in the same electrochemical cell, are being studied but still show unsatisfactory performances [32]. Combining electrolysis and fuel cell in two distinct devices has instead become competitive for seasonal storage of RES due to its high energy density, low maintenance, very low self-discharge and no toxic emissions or noise. However, the overall efficiency is lower than batteries and much concern is related to storage methods, given hydrogen's low volumetric density [8, 20, 24].

- *Synthetic natural gas (SNG)* production from renewable H_2 and CO_2 has gained much attention since it combines RES and CO_2 capture from the atmosphere. Here a second step is required beyond water electrolysis: methane

synthesis from hydrogen and carbon dioxide in a methanation reactor, which requires high temperatures (150-550°C [33]). The SNG, composed mainly by methane, has high volumetric density and can be used for domestic heating, fed into the gas grid or re-converted to electricity in a turbine, with an overall power-to-power efficiency of < 35%. However it is not a carbon free option, since whatever process the SNG undergoes after production emits CO_2 [14, 34, 35].

1.3.4. Mechanical energy storage

In mechanical applications, electricity is stored as kinetic or potential energy using mechanical processes as pumping, compression, expansion, acceleration or deceleration. Flywheels, that exploit the angular momentum of a spinning mass, offer short discharging rates and are used for faster operations [16, 20]. Longer duration mechanical technologies are, instead, pumped hydro and compressed air:

- *Pumped hydro storage (PHS)* takes advantage of the potential energy difference between two water reservoirs at different levels. Water is pumped to the upper reservoir during charging, while it flows down through a turbine to generate back electricity. Its capacity is proportional to the quantity of water available and height difference between the natural reservoirs, therefore this technology is highly site-dependent. It usually has long lifetime and low cycle cost, but the drawbacks include huge investment costs and environmental impact [8, 16, 18, 20]. It is the most mature storage technology and currently provides around 95% of global installed capacity [36] and it is employed for large scale storage [20].
- *Compressed air energy storage (CAES)* accumulates energy by mechanically compressing air in natural or artificial caverns. Like PHS, CAES is also site-dependent, as it needs a suitable underground location and to be close to a gas turbine plant, where high-pressured air is expanded for power generation. This application has high power capacity, long energy storage duration and low capital cost. On the other hand, it has low energy density and is not carbon-free as it requires fuel combustion in the expansion phase [8, 20, 37, 38]. A promising improvement of this technology is the Advanced Adiabatic CAES, where thermal storage is integrated to store heat, avoiding combustion and increasing efficiency [38].

For the sake of completeness, Table 1.2 summarizes the technical characteristics of each technology while Table 1.3 provides an overview their indicative capital costs and maturity, as found in recent literature.

Type	Technology	Power rating	Discharge time	Energy density	Efficiency	Cycle life	Lifetime	Self discharge
		MW		*Wh/kg*	*%*	*cycles*	*years*	*%/day*
Electrochem.	**Lead-acid**	0-20	sec-h	25-50	65-80	200-1800	3-12	0.1-0.3
	NiCd	0-40	sec-h	50-75	60-70	200-3500	10-20	0.2-0.6
	NiMH	0.1-1	h	70-80	65-70	50-1800	15	0.4-1.2
	NaS	0.15-10	sec-h	150-240	75-90	2500-4500	10-15	0.05
	NaNiCl	0-0.3	sec-h	100-120	90	2500	10-14	5
	Li-ion	0.1-50	min-h	75-200	90-99	1000-10k	5-20	0.1-0.3
	Metal-air	0-1	sec-days	110-650	50-65	100-300	0.17-30	0-0.01
Flow batteries	**VRB**	0.3-15	sec-days	10-50	75-85	12k-14k	5-20	0.15
	ZBR	0.05-10	sec-10h	30-60	60-80	2000-10k	5-20	~ 0
	PSB	0.1-15	sec-10h	20-30	60-75	2000	10-15	~ 0
Chemical	**Hydrogen**	< 50	sec-days	800-10k	20-50	> 20k	5-20	~ 0
	SNG	1-100	h-days	10000	20-50	-	30	~ 0
Mechanical	**PHS**	100-5000	h-days	0.5-2	65-85	10k-30k	30-60	0.01
	CAES	5-300	h-days	30-60	70-80	8000-12k	20-40	0.5

Table 1.2: Technical characteristics overview of energy storage technologies [8, 16, 20]

Type	Technology	Power cost	Energy cost	Maturity
		€/kW	*€/kWh*	
Electrochem.	**Lead-acid**	240-480	120-400	Mature
	NiCd	400-1200	320-1900	Mature
	NiMH	480-1450	160-1440	Commercialized
	NaS	800-2400	240-400	Commercialized
	NaNiCl	120-240	80-275	Commercialized
	Li-ion	960-3200	480-3200	Commercialized
	Metal-air	1400-1520	8-280	Developing
Flow batteries	**VRB**	480-1200	120-1200	Developed
	ZBR	320-2000	270-1000	Developed
	PSB	560-2000	120-800	Developing
Chemical	**Hydrogen**	400-8000	1.5-12	Developing
Mechanical	**PHS**	400-3700	4-345	Mature
	CAES	320-640	30-120	Commercialized

Table 1.3: Estimated cost and maturity level overview of energy storage technologies [8]

1.3.5. Suitability assessment

For each of the technologies described above, compatibility with the requirements is assessed in Table 1.4.

Type	Technology	Discharge time	Rated power	Lifetime	Cycle life	Environ. friendly	Site-independent
		>8 h	*>50 kW*	*>20 yrs*	*>7300*		
Electrochem.	**Lead-acid**	•					•
	NiCd	•		•			•
	NiMH	•				•	•
	NaS	•			•	•	•
	NaNiCl	•					•
	Li-ion	•	•	•	•	•	•
	Metal-air	•		•		•	•
RFB	**VRB**	•		•	•	•	•
	ZBR	•		•	•		•
	PSB	•					•
Chemical	**Hydrogen**	•	•	•	•	•	•
	SNG	•	•	•			•
Mechanical	**PHS**	•	•	•	•	•	
	CAES	•	•	•	•		

Table 1.4: Matrix of application requirements of energy storage technologies to residential grid-connected systems (data from Table 1.2)

From the table we can deduce that:

- Hydrogen fuel cell systems and Li-ion batteries are the most promising technology from a technical, environmental and logistic point of view
- Vanadium and Zinc-Bromine redox flow batteries lack in power capacity, which however is easily scalable in this type of technology, therefore are considered suitable as well
- Electrochemical batteries (excluding Li-ion) show some technical and environmental dearths, while polysulfide RFB doesn't meet many of the requirements
- Synthetic natural gas is excluded as it is not carbon-free
- Pumped hydro and compressed air are excluded as it is unlikely that they can be physically placed near residential areas

Because of their maturity, several technical and economic models about the applications of electrochemical batteries (excluding RFB) in residential PV-storage systems are already present in literature [22, 39–41]. NiMH and Li-ion batteries have shown the highest potential for their technical features, although their capital cost is high [22, 41], while lead-acid batteries have been extensively investigated from an economic point of view due to their lower initial cost, showing good profitability [40].

The global demand for batteries is set to increase of 14 times by 2030, leading to an equivalent increase in demand for raw materials and possible waste, with significant consequences for the environment [42]. Li-ion batteries are especially concerning, given the growing employment - in portable electronics, electric vehicles and industrial applications - and small recycle rate (<5% [43]). This issue lead the European Commission to recently update its legislation on batteries, imposing new guidelines on sustainability and safety to reduce their environmental impact [44].

In view of the abundance of comprehensive studies on electrochemical batteries with respect to other technologies, and acknowledging the concerns behind the new European regulations which mainly involve those devices, this work will rather focus on novel and equally promising alternatives. Hydrogen systems and redox flow batteries are newer and still developing technologies with strong potential for residential applications, as showed in Table 1.4, and will therefore be the focus of this thesis.

1.4. Research question and approach

1.4.1. Problem statement

The great diffusion of distributed PV on house rooftops has not yet been followed by an increased request of energy storage solutions. Excluding pumped hydro storage, which is extensively used in large scale applications, a few commercial options available nowadays for smaller scales are conventional electrochemical batteries, mainly lead-acid and lithium ion. However, a comprehensive literature study highlighted the great potential of some novel technologies, that could soon become efficient, reliable and affordable ESS, providing benefits for the consumers, the energy market and the environment.

The aim of this thesis project is to study the performance of novel storage technologies for a household and neighbourhood residential system equipped with PV. At different self-consumption rates, the optimal sizing of both PV and storage will be determined and an economical analysis will be performed to check if the investment is profitable or not.

1.4.2. Research question

The present work will therefore attempt at answering the question:

Are novel kinds of energy storage, like redox flow batteries and hydrogen, economically feasible for application in residential household or neighbourhood PV systems?

The subquestions that need to be answered in order to accomplish to the main objective are the following:

- *How much is the energy mismatch between a typical household energy consumption and rooftop PV production?*
- *What are the working principles of these technologies? How can they be modeled and coupled to the PV-household system?*
- *How much is the estimated current and future market price of these technologies?*
- *How high should the self-consumption level be in order observe the benefits of a storage system?*
- *Is the cost of such a system convenient? What can be done in the future to make it feasible?*

1.4.3. Approach

In order to accomplish the thesis goal, the work has been structured as follow:

- Literature study of storage technology options and their benefits of to grid-connected systems
- Evaluation of the residential energy mismatch
- Study of the storage technologies working principle and implementation in a MATLAB Simulink model
- Setup of a Mixed Integer Non Linear optimization problem (MINLP) in GAMS to optimize the system size at minimum cost
- Collection of simulation outputs
- Interpretation and discussion of results

1.5. Document outline

The research question in this thesis is studied and developed in five sections, each corresponding to a chapter. After a research on current solutions or storage for the grid presented in this chapeter, the theoretical and commercial features of each component of the system are presented in Chapter 2, where a literature study is accompanied by the implementation of a MATLAB model. Then, Chapter 3 provides a detailed explanation of the procedure employed to size and optimize the considered residential power systems. Afterwards, in Chapter 4, a comprehensive costs analysis for the various devices is given. Successively, Chapter 5 collects and discusses the results of the optimization model. Finally, Chapter 6 shows the author's conclusions and recommendations.

2
Model

2.1. Purpose

In order to determine the feasibility of different storage technologies in a residential PV-load system, it is important to first understand the theory and working principles behind each component. This was done with the help of a MATLAB Simulink model, in which each device is modelled starting from their theoretical principles, and developed according to experimental data found in the literature and commercially available options. This ensures that the equations and parameters used later in the optimization are validated and represent the behaviour of commercially available devices as accurately as possible.

2.2. Structure

The model proposed for this project aims at reproducing the behaviour of a real residential system with PV generation and grid connection, to which a storage system is added. In such a system, 5 components can be distinguished:

- **Load**: A single house or a small neighbourhood that consumes electricity
- **Generator**: Photovoltaic panels for local renewable power generation
- **Storage**: The storage system, object of the study
- **Grid**: A connection point to the main grid
- **Control**: A local controller for power balance and operation management

The model is built in MATLAB Simulink (version 2021a) and made up of a main Simulink block-diagram, containing blocks and connections that represent the subunits of the system (Figure 2.1), plus an input script to initialize the simulation. The block-diagram is composed by 4 blocks representing load, generation, storage and grid, while the control role is assumed by the links and operations connecting the blocks. Information about power flow are exchanged between each block in form of digital signals along connections performing power balance at every timestep, in the way outlined in Figure 2.2.

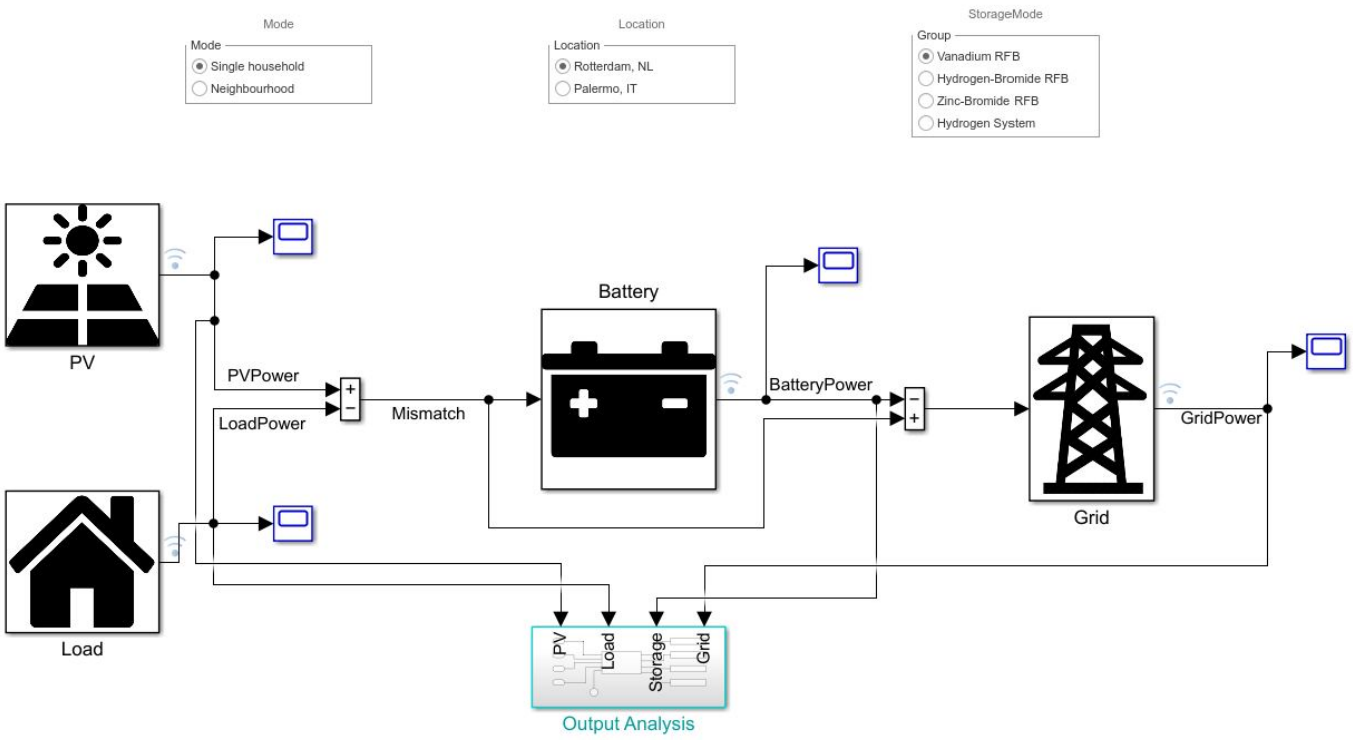

Figure 2.1: Appearance of the system model in Simulink

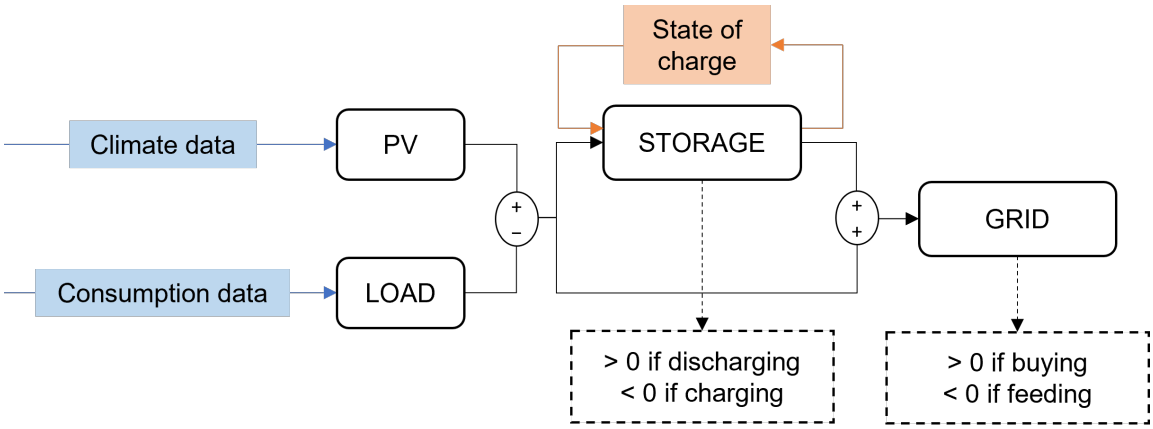

Figure 2.2: Structure of the system model

Outside the blocks, information is exchanged as power in Watts. The convention adopted here attributes the positive sign to power produced from the component, and the negative sign to power consumed or stored by the component. Inside the blocks, different sub-systems, equations and operations are used to model the behaviour of the component, as explained in the following paragraphs.

The model runs for 35040 discrete timesteps, corresponding to one year in 15 minutes resolution (365*24*4 = 35040). This research focuses on seasonal storage, which is only minimally affected by fluctuations in the order of less than hours, therefore a 15 minutes timestep duration was chosen as it gives sufficient precision

in the PV generation and house consumption representations, but also reasonable computation time. Moreover, it is assumed that the PV system is equipped with a small battery for frequency regulation, therefore small fluctuations in solar irradiance can be neglected.

The behaviour of a storage device primarily depends on the load consumption versus PV production, i.e. the energy mismatch. In order to provide a sufficiently complex and general analysis, the model simulates different scenarios that vary according to:

Rotterdam, NL	<	**Location**	>	Palermo, IT
Single house	<	**House type**	>	Neighbourhood of 10 houses
Gas heating	<	**Heating type**	>	Electric heating

One northern and one southern Europe location were chosen in order to observe the behaviour at different sunshine durations and intensities. Moreover, it is useful to study how such a system would work in a single independent house rather than in a neighbourhood with partially shared and centralized energy consumption. Heating is an important consuming item in a house, and the current trend foresee a transition from gas boilers to electric devices, with a huge impact on the electricity consumption. This alternative is considered in the model as well.

Before the storage technologies analysis, a description on how the load, PV and grid blocks have been modeled is given in the following sections.

2.2.1. Load block

The load consumption profile is a crucial element as it determines the sizing of the system. It is taken as a fixed and independent parameter in the model, and all the simulation is executed starting from it.

Yearly electricity consumption profiles for single houses and neighbourhoods in the two locations were obtained using the behaviour-based open source software called *LoadProfileGenerator* [45]. On top of the default parameters already included in the software, historical temperature profiles (the same used for PV) were added for accurate heating and cooling calculation. A predefined "2 children, 2 parents, 1 working, 1 working at home" household type was used for the single house mode simulation, while a heterogeneous set of 10 different households types was chosen for the neighbourhood mode.

Some features worth mentioning are:

- **Heating/cooling**: In gas mode, no cooling is considered in Rotterdam, while some electric cooling (fans, air conditioners) is assumed for Palermo. On the other hand, in electric heating mode, a continuous flow heat pump with COP 3 is used for both locations. These differences are observable by comparing the energy consumption totals in Figure 2.3.

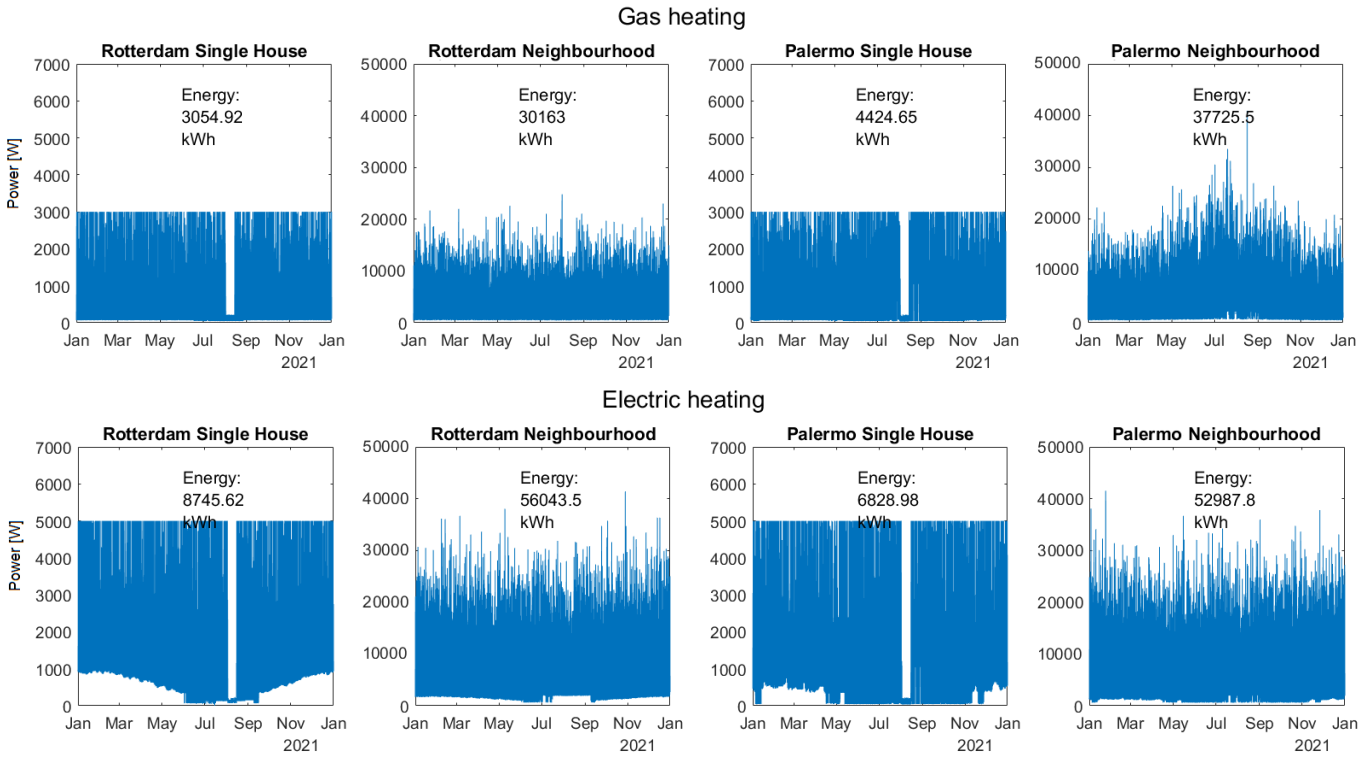

Figure 2.3: Yearly load profiles of the 8 electricity consumption scenarios analysed

- **Power cutoff**: Single house profiles are cut to 3 kW in gas mode and 5 kW in electric heating mode, according to the limitations imposed by the DSO to avoid dramatic electricity demand peaks at certain hours of the day. This cut is not visible in neighbourhood profiles as all the single households hardly ever reach the maximum power at the same time.
- **Holidays**: A period where the house owners are out of their home for holidays is foreseen by the software around August, as can be seen in figure. This is particularly important to consider for seasonal storage.

2.2.2. Photovoltaic block

Local energy generation is performed by photovoltaic panels on the houses rooftops. These are modelled starting from typical climate data, which is elaborated to obtain the power output. Typical yearly profiles of the main meteorological indicators for PV performance - namely solar irradiance, air temperature and wind speed - are extracted from climate databases. Taking average profiles ensures that neither an exceptionally favourable nor an unfavourable year is considered, providing a more generic result. On the other hand, neglecting these anomalies could lead to unrealistic conclusions: this factor must be taken into account, especially when increasing the self-consumption of the PV-storage system.

Weather data for Rotterdam is taken from the Dutch PV Portal database [46], which

collects meteorological data measured by the Royal Netherlands Meteorological Institute (KNMI). Whereas, data for Palermo is taken from the Typical Meteorological Year tool of the EU Photovoltaic Geographical Information System [47].

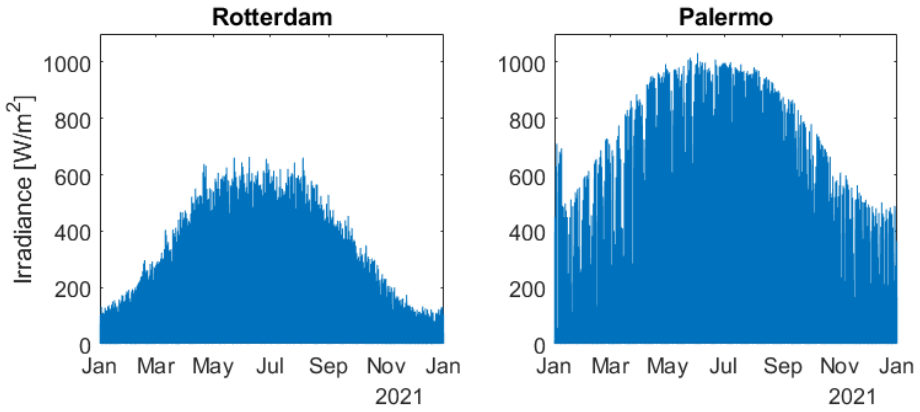

Figure 2.4: Average yearly irradiance profiles in Rotterdam and Palermo

The power produced by typical crystalline silicon (cSi) photovoltaic panels can be calculated as:

$$P_{\text{PV}} = \eta(G_M, T_M) \cdot G_M A \tag{2.1}$$

where P_{PV} is the panel output power [W], η is the overall efficiency which depends on meteorological factors, G_M is the irradiance incident to the module (approximated to the global horizontal irradiance, assuming that the module is at a 90° angle of incidence at any time) and A is the panel area [m^2].

The overall efficiency η at every level of irradiance and temperature is calculated by Lorenz et al. [48] as:

$$\eta(G_M, T_M) = \eta_{\text{st}}(G_M, 25\,°\text{C}) \cdot [1 + \alpha(T_M - 25\,°\text{C})] \tag{2.2}$$

where η_{st} is the efficiency at standard temperature (25°C) taken as 19.2% for typical cSi, α is a temperature coefficient taken as 0.0035 /°C for cSi [48], and T_M is the module temperature [°C] calculated using the Sandia model [49]:

$$T_M = I \cdot \exp\left(a + b \cdot v_{\text{wind}}\right) + T_{\text{amb}}, \quad a = -3.2, \quad b = -0.05675 \tag{2.3}$$

where a and b are parameters relative to the construction, materials and mounting configuration of the module, while T_{amb} and v_{wind} are respectively the ambient temperature [°C] and wind speed [m/s] taken from the databases.

2.2.3. Storage block

The storage block is the most complex one and it represents the heart of this study. Redox flow batteries, electrolysers and fuel cells are all electrochemical devices, and their behaviour can be modelled in the same way, only varying some numeric parameters. First, an overview of the theory behind electrochemical devices is provided, then how each type is modelled is explained.

The electrochemical cell

Electrochemical devices essentially consist of the same unit element: the electrochemical cell. Electrochemical cells are of two types: voltaic (or galvanic) cells, in which chemical reactions are used to produce electrical energy, and electrolytic cells, where electrical energy is used to bring forward chemical reactions. A cell consists of two electrodes (electrically conducing plates) separated by an electrolyte (ionically conducting solution), and is split in two half cells, connected by an external electrical circuit that enables production or use of electricity. The half-cells are usually separated by a membrane that allows ionic transport but maintains electrical insulation [50, 51]. A schematic representation of a galvanic and electrolytic cell is given in Figure 2.5.

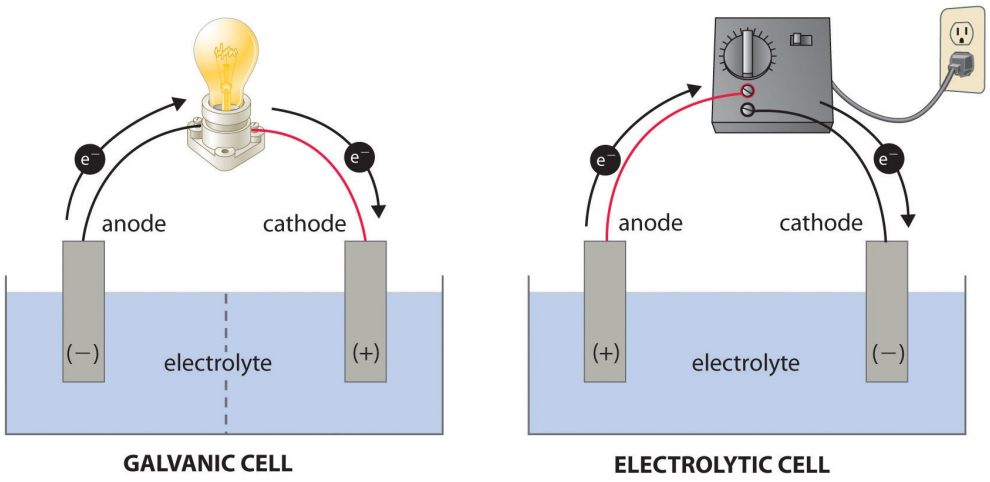

Figure 2.5: Schematic representation of a galvanic and an electrolytic cell [52]

The reactions occurring at the electrodes are called reduction-oxidation (Red-Ox) reactions and involve transfer of electrons from one substance to another. After the oxidation process that occurs at the negative electrode (anode), the released electrons pass through an external electrical circuit and arrive at the positive electrode (cathode), where the reduction process occurs. The generalized reactions are:

$$\begin{aligned} &\text{Oxidation:} && \text{Ox}^{(m-n)+} && \rightarrow && \text{Ox}^{m+} + ne^- \\ &\text{Reduction:} && \text{Red}^{p+} + ne^- && \rightarrow && \text{Red}^{(p-n)+} \\ &\text{Overall:} && \text{Ox}^{(m-n)+} + \text{Red}^{p+} && \rightarrow && \text{Ox}^{m+} + \text{Red}^{(p-n)+} \end{aligned} \tag{2.4}$$

where m and p represent oxidation numbers and n is the number of exchanged electrons.

Different chemical species are associated to different voltages according to the potential difference developed at the interface between the electrode and the electrolyte. By convention, the standard hydrogen electrode (SHE) is defined to have a potential of 0 V, and all the other electrodes assume negative or positive values with respect to this reference. The electric potential of a cell depends on the redox

couple used. The overall cell potential at standard conditions equals the difference between the cathode and anode potentials:

$$V_{\text{cell}} = V_{\text{anode}} - V_{\text{cathode}} \tag{2.5}$$

From a thermodynamic point of view, the cell potential is an expression of the change in Gibbs free energy ΔG, and their relation is given by:

$$\Delta G_{\text{cell}} = -nFV_{\text{cell}} \tag{2.6}$$

where n is the number of exchanged electrons and F is the Faraday constant. The sign of Gibbs free energy change describes the spontaneity of a process, therefore a positive V_{cell} ($\Delta G_{\text{cell}} < 0$) corresponds to a galvanic cell, while a negative V_{cell} ($\Delta G_{\text{cell}} > 0$) characterizes an electrolytic cell.

At standard conditions (T = 298 K, P = 1 atm, C = 1 M), the cell open circuit potential can be simply calculated from Eq. 2.5 using standard electrode potentials tables. However at different conditions, the influence of temperature, pressure and concentration should be taken into account using the Nernst equation:

$$V_{\text{cell}} = V^{\circ}{}_{\text{cell}} - \frac{RT}{nF} \ln \frac{a_{\text{red}}}{a_{\text{ox}}} \tag{2.7}$$

where R is the ideal gas constant, T is temperature, n is the number of exchanged electrons, F is the Faraday constant and a are the activities of reduced and oxidized species (for ideal mixtures, activity can be expressed as molar concentration for liquids or partial pressure for gases).

The Nernst equation calculates the cell open circuit voltage (OCV), i.e. the theoretical electromotive force at zero current, the maximum achievable voltage for galvanic cells and or the minimum necessary voltage for electrolytic cells. Increasing current, the electrochemical process starts to develop some losses, that decrease the available potential in galvanic cells or increase the needed potential in electrolytic cells. The difference between this new voltage and the OCV is defined as overpotential $\eta = V - V_{\text{OCV}}$. Consequently, the current flow in the electrodes will depend on the applied overpotential.

Losses in an electrochemical device can be visualized by plotting the current-voltage (i-V) relation as in Figure 2.6. The main types are:

- Activation losses, due to the double layer effect that creates an energy barrier at the electrode-electrolyte interface, requiring some extra activation energy to kickoff both spontaneous and induced electrochemical processes.
- Ohmic losses, due to the electrical resistance of electrolyte, wires and current collectors.
- Mass transport losses, due to the resistance to diffusive transport of mass, which is more pronounced at high current densities.

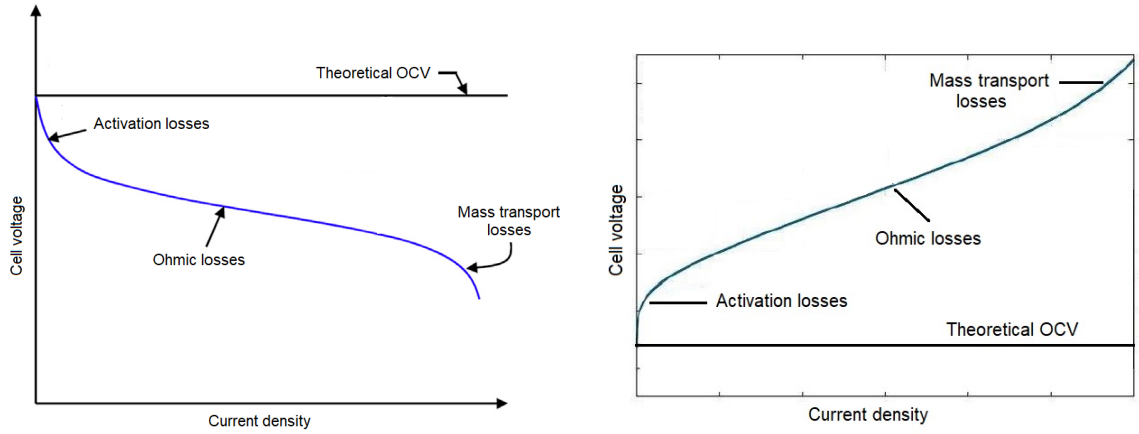

Figure 2.6: Typical i-V curves for a galvanic (left) and electrolytic (right) cell

The complete expression of potential for a galvanic cell therefore becomes:

$$V = V_{\text{OCV}} - \eta_{\text{ohmic}} - (\eta_{\text{act}} + \eta_{\text{trans}})_{\text{an}} - (\eta_{\text{act}} + \eta_{\text{trans}})_{\text{cat}} \tag{2.8}$$

where each overpotential depends on current density in different ways. For electrolytic cells, the equation is the same with opposite η signs.

Some redox reactions (like the hydrogen and oxygen evolution reactions) require an electrocatalyst, a catalytic substance used as electrode or placed on the electrode surface that increases the rate of the electrochemical reaction. This is often an expensive metal or compound, which increases the overall device cost.

Electrochemical model

To simulate the behaviour of an electrochemical storage device, the literature proposes different types of algorithms with various levels of complexity. A steady state model based on the most important equations relative to the technology is employed for this research, inspired by the Vanadium RFB model developed by Blanc et al. [53]. The main losses are accounted for in the algorithm according to the following assumptions:

- Electrical conduction and ionic diffusion losses are considered Ohmic resistance, whose value is extrapolated from recent experimental studies
- An overpotential is included, whose value is extrapolated from recent experimental studies
- Losses due to shunt currents are significant only at relatively high current densities, that are not necessary in this model. Any other stack-related loss is neglected.
- Losses due to pumps are calculated or estimated in percentage loss depending on the type of storage technology.
- Losses due to inverters are inserted with a total efficiency of 96%.

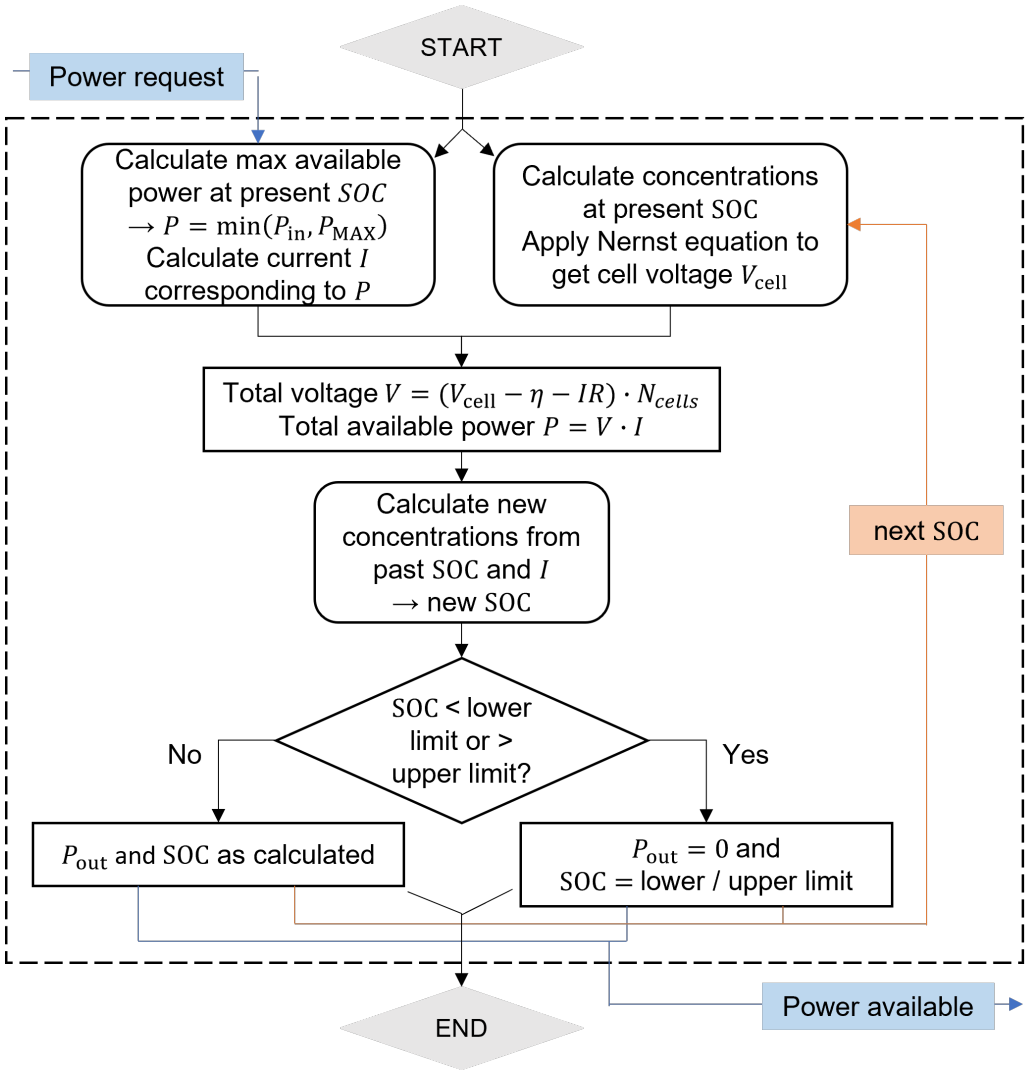

Figure 2.7: Flow chart of the storage block in the Simulink system model

The algorithm works as follows:

1. The first block reads the power requested from the central controller. First, it compares it to the maximum available power relative to the present state of charge. Then, the corresponding current is calculated through a 2^{nd} order function of power and SOC. Both functions are interpolated from experimental data obtained from literature.

2. In the second block, concentrations of the chemicals reacting in the cell are determined from the SOC, and the Nernst equation is applied to calculate the open circuit cell potential. Then, the total voltage is calculated as

$$V = (V_{\text{cell}} - \eta - IR) \cdot N \tag{2.9}$$

where η is the overpotential [V], R is the Ohmic resistance [Ω] and N is the number of cells in the battery. Finally, the available power is $P = V \cdot I$.

3. Then, some calculations in preparation for the next timestep are performed. The new concentrations depend on the current I, the electrolyte volume Vol and the flow rate Q [53]:

$$C_{\text{new}} = C_{\text{prev}} \pm \frac{N}{VolF} \cdot I\Delta t \pm \frac{N}{2FQ} \cdot I \tag{2.10}$$

   where F is the Faraday constant and Δt is the timestep duration. Hence, the new SOC can be calculated. If its value falls outside the predefined limits, meaning the battery is either too charged or too empty, the algorithm sets the output power to zero and leaves the SOC unchanged.

A few parameters (number of cells, membrane area and electrolyte tanks volume) need to be set before starting the simulation, depending on the technical specification of the battery used. The two most important ones are the number of stacks and the electrolyte or gas product volume, respectively linked to the rated power and energy capacity of the battery.

During the simulation, at each timestep the sign of power request tells the algorithm to proceed along one of the two "symmetrical" roads corresponding to charge (positive) or discharge (negative). At the end, the model is able to provide useful information on voltage, current, power and state of charge profiles, and to calculate the overall system efficiency.

2.3. Redox flow batteries

A redox flow battery (RFB) is a special type of electrochemical storage device, where electrolytes are stored in separate tanks and flow into the cell stack with the help of pumps. Power is generated/consumed when the electrolytes flow through the cell anode and cathode chambers, separated by an ion-exchange or microporous membrane, and undergo electron-transfer reactions at inert electrodes [29, 30]. The main advantage of RFB is their ability to decouple rated power from energy storage capacity, unlike common batteries where the two are intimately linked. This advantage provides a considerable flexibility, as the power output is controlled by the size of the cell stack, while the volume of the electrolyte tanks defines its energy capacity [16].

Various metal-based redox couples have been studied over the past few decades. Among them, all-vanadium RFB (VRFB) and hybrid zinc-bromine (ZBFB) flow batteries are the most investigated ones, while the hydrogen-bromine (HBFB) is being studied as a combination between a fuel cell and a redox battery.

2.3.1. Vanadium redox flow battery

The all-vanadium redox flow battery (VRFB) is the most successful among RFB and the only one that has reached effective commercial fruition [54]. Its operation is based on the ability of vanadium to exist in solution in four different oxidation

states. Vanadium ions are used at both compartments, namely VO^{2+} and VO_2^+ in the positive electrolyte (catholyte) and V^{2+} and V^{3+} in the negative electrolyte (anolyte). The electrochemical produced by these solutions in the cells are:

$$\begin{array}{lrcll} \text{Anode:} & V^{2+} & \rightarrow & V^{3+} + e^- & V_{an} = -0.26\,\text{V} \\ \text{Cathode:} & VO_2^+ + 2H^+ + e^- & \rightarrow & VO^{2+} + H_2O & V_{cat} = 1.00\,\text{V} \\ \text{Overall:} & V^{2+} + VO_2^+ + 2H^+ & \rightarrow & V^{3+} + VO^{2+} + H_2O & V_{cell} = 1.26\,\text{V} \end{array} \tag{2.11}$$

where the arrows are in direction of discharge. The battery consists of two closed electrolyte circuits containing the vanadium ions solutions, which flow from two separate containers through an electrochemical cell in each side of the membrane, as shown in Figure 2.8.

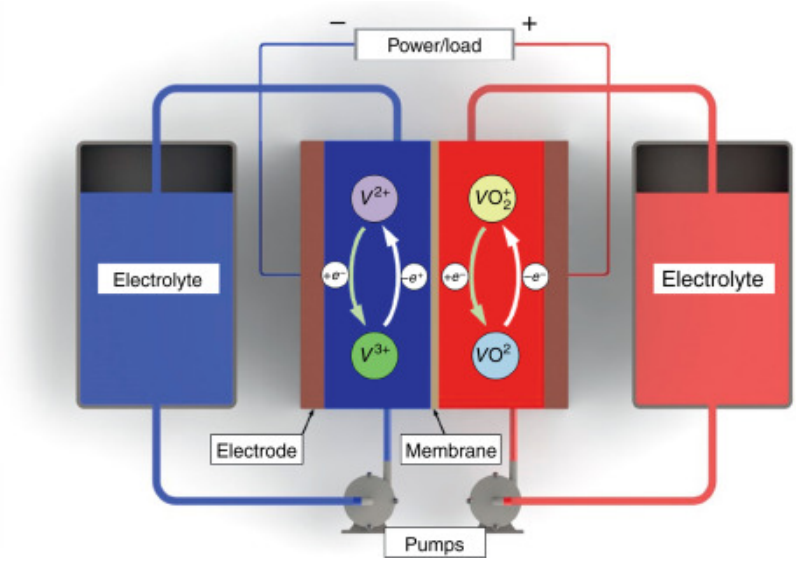

Figure 2.8: Schematic representation of a VRFB [29]

The state of charge for this battery can be calculated as [53]:

$$\text{SOC} = \frac{[V^{2+}]}{[V^{2+}] + [V^{3+}]} = \frac{[VO_2^+]}{[VO_2^+] + [VO^{2+}]} \tag{2.12}$$

This technology has already been studied for some years and is already commercialized by companies worldwide. A list of the main commercial options and relative manufacturers is given in Table 2.1.

Source	Manufacturer	Model	Stack Voltage [V]	Rated Current [A]	Rated Power [kW]	Capacity [kWh]	Efficiency [%]
[55]	H2 Inc.	EnerFlow 330			5-10	60	
[56]	Volteiron	powerRFB	40-64		10	13	
[57]	Golden Energy C.	GEC-VFB		210	10	30	75
[58]	VFlowTech	POWERCUBE			10	100	85
[59]	UniEnergy Tech.	ReFlex™	42-67	350	14	45	76-84
[60]	VisBlue		40-60		5-100	25-500	70
[61]	Big Pawer		48-77	210	10	50	> 75
[62]	Pinflow	PFS	30-70	170	30	150	< 80
[63]	StorEn Tech.	TitanStack	48	105	50	500	70-80
[64]	Rongke Power	Vmodule1-B	200-310	150	50	200	65-75
[62]	Pinflow	PFM	30-70	170	60	300	< 80
[55]	H2 Inc.	EnerFlow 430			75	385	
[62]	Pinflow	PFL	30-70	170	200	600	< 80
[65]	Sumitomo Electric				250	750-1500	
[66]	Cell Cube	FB 250 - 1000			250	1000	
[66]	Cell Cube	FB 500 - 2000			250	2000	
[66]	Cell Cube	FB 500 - 2000			500	2000	
[67]	Largo Clean Energy	VCHARGE±6	500-800		1000-1200	6000	78
[67]	Largo Clean Energy	VCHARGE±8	500-800		1000-1200	8000	78
[67]	Largo Clean Energy	VCHARGE±10	500-800		1000-1200	10000	78

Table 2.1: Technical specifications of commercially available VRFB [55–67]

Due to the nature of this battery, depending on SOC the OCV ranges from 1.1 V to 1.6 V [54]. Several cells are connected in series to form a stack, so as to produce and store higher potential. The typical current density of commercial VRFBs is in the order of 80–100 mA/cm^2 and correspondingly the power density reaches 100 mW/cm^2, however enhancements were found in experimental studies with improved architecture [68], proving that there is room for future development. Although they present lower energy efficiency than most conventional batteries (65-80%), VRFB are particularly competitive for stationary systems and long storage times (such as seasonal storage) for their energy capacity scalability, extremely low self-discharge, fast response, ambient temperature operation and long cycle and service life.

Electrolyte pumps play an important role in the battery operation and also in the overall efficiency. Losses due to pumps are estimated to be 2-3% [69] of the total energy efficiency. Moreover, since the residential system works in AC, two inverters are required, whose total efficiency is usually around 93% [70].

In accordance to experimental data from recent studies reported in the literature [53, 69, 70] and considering the technical specifications of commercial options, the

vanadium battery model has the parameters and behaviour showed in Table 2.2 and Figure 2.9.

VRFB			
V_{cell}	1.26 V	Cell area	3000 cm^2
Charge R	0.0009 Ω	Discharge R	0.0008 Ω
Charge η	0.001 V	Discharge η	0.001 V
Charge nominal i	0.083 A/cm^2	Discharge nominal i	0.067 A/cm^2
Charge nominal power d.	0.13 W/cm^2	Discharge nominal power d.	0.08 W/cm^2
Depth of discharge	0 - 100 %	Auxiliary losses	6.50 %
Electrolyte max concentration	2 M (all vanadium iones)		

Table 2.2: Summary of model parameters for the VRFB (validated against experimental data)

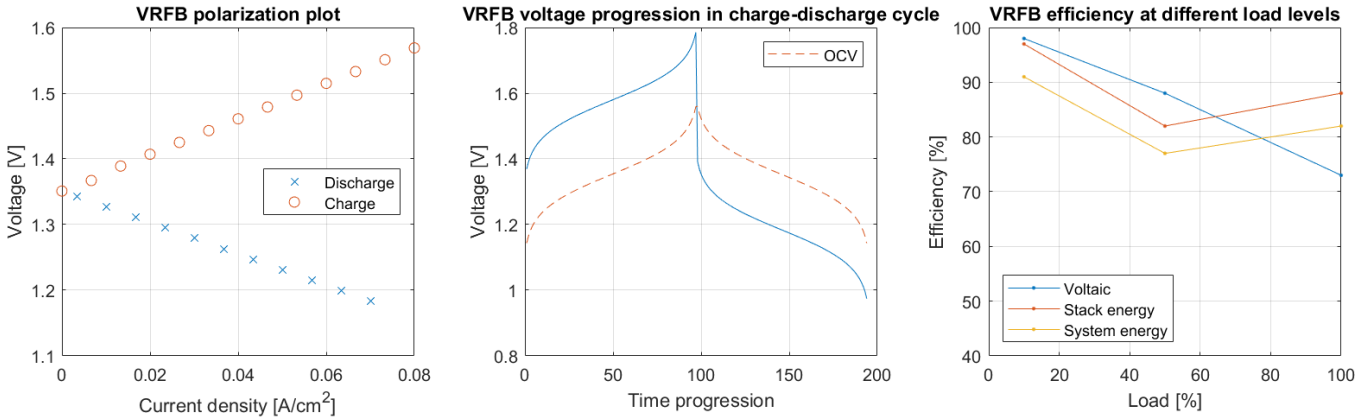

Figure 2.9: Polarization curve (left), voltage progression in charge-discharge cycle (centre), and efficiencies (right) of a VRFB (validated against experimental data)

2.3.2. Hydrogen-bromine redox flow battery

The hydrogen/bromine flow battery (HBFB) is a promising alternative to the conventional redox flow batteries, that reported excellent electric-to-electric efficiency. Its operating principle can be described with a typical cell structure and the reactions in discharge direction are [71]:

$$\begin{array}{lrcll} \text{Anode:} & \text{H}_2(\text{g}) & \rightarrow & 2\text{H}^+ + 2e^- & V_{\text{an}} = 0.00\,\text{V} \\ \text{Cathode:} & \text{Br}_2 + 2e^- & \rightarrow & 2\text{Br}^- & V_{\text{cat}} = 1.09\,\text{V} \\ \text{Overall:} & \text{H}_2(\text{g}) + \text{Br}_2 & \rightarrow & 2\text{HBr} & V_{\text{cell}} = 1.09\,\text{V} \end{array}$$

It is different from the VRFB as two reactants are in gas form (hydrogen and bromide), and one of them is not stored in solution but needs a compressed tank. The state of charge for this battery is calculated based on the concentration of Br_2 dissolved in water. Other than the inverters, this system requires two circulating pumps/compressors and a cooling system to avoid heating. The losses due to

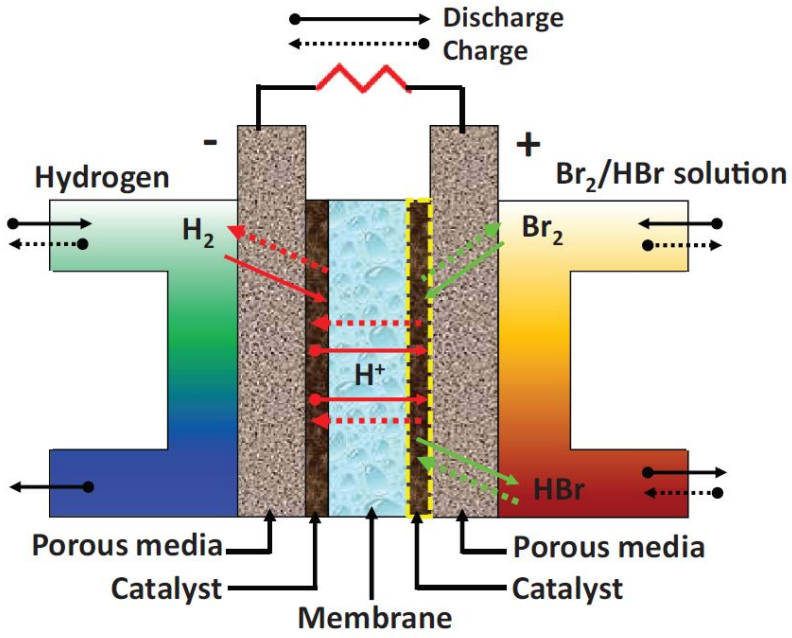

Figure 2.10: Schematic representation of a HBFB [72]

these components are estimated respectively at 2% and 3% [73].

This technology is currently being proposed commercially by a Dutch company named Elestor [74]. The technical features of their battery include:

Sources	Manufacturer	Rated Power [kW]	Capacity [kWh]	Efficiency [%]	N° of stacks	H_2 tank volume [m^3]
[74]	Elestor	200	2000	65-75	25	45

Table 2.3: Technical specifications of commercially available HBFB [74]

The hydrogen-bromine battery parameters and behaviour are showed in Table 2.4 and Figure 2.11, according to the literature [71, 72] and Elestor's specs [74].

HBFB			
V_{cell}	1.09 V	Cell area	100 cm^2
Charge R	0.002 Ω	Discharge R	0.004 Ω
Charge η	0.05 $\cdot i$ V	Discharge η	0.05 $\cdot i$ V
Charge nominal i	1 A/cm^2	Discharge nominal i	1 A/cm^2
Charge nominal power d.	0.80 W/cm^2	Discharge nominal power d.	0.50 W/cm^2
Depth of discharge	10 - 90 %	Auxiliary losses	9 %
Electrolyte max concentration	4 M (Br_2), 2.8 M (HBr)		

Table 2.4: Summary of model parameters for the HBFB (validated against experimental data)

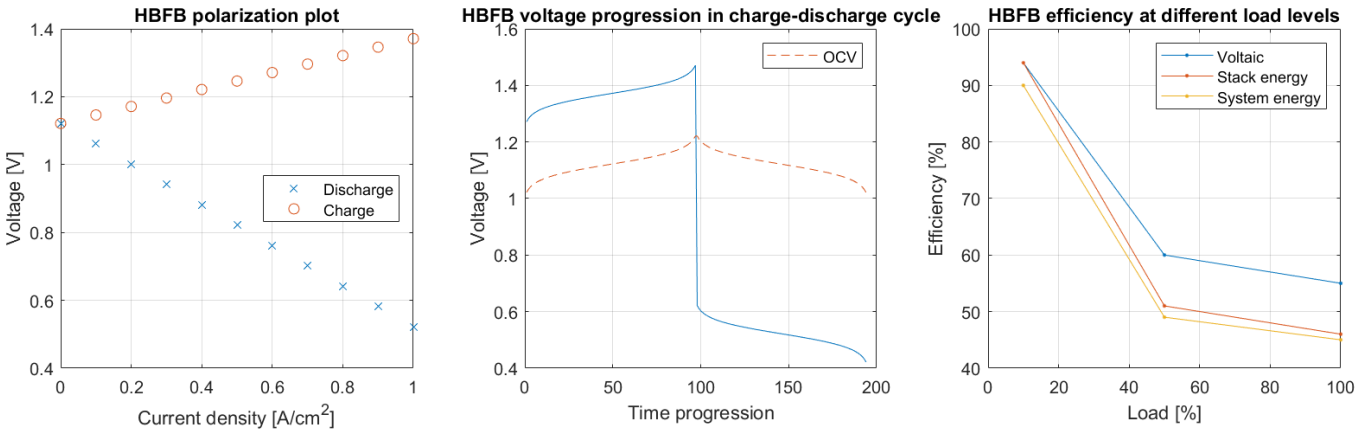

Figure 2.11: Polarization curve (left), voltage progression in charge-discharge cycle (centre), and efficiencies (right) of a HBFB (validated against experimental data)

2.3.3. Zinc-Bromine redox flow batteries

The $Zn - Br_2$ flow battery is actually an hybrid between a flow and a conventional battery, because part of the energy is not stored in electrolytic solution contained in a separate tank, but rather as a solid layer of zinc coating the electrode, located in the stack [16]. During charge, a thin layer of metallic zinc is electrodeposited at the carbon-based negative electrode with the simultaneous oxidation of bromide ions to bromine at the positive electrode. During discharge, the battery relies on the inverse reactions. The half cell reactions in discharging direction are [75]:

$$\begin{array}{lrcll} \text{Anode:} & Zn & \rightarrow & Zn^{2+} + 2e^- & V_{an} = -0.76\,V \\ \text{Cathode:} & Br_2 + 2e^- & \rightarrow & 2Br^- & V_{cat} = 1.09\,V \\ \text{Overall:} & Zn + Br_2 & \rightarrow & ZnBr_2 & V_{cell} = 1.85\,V \end{array} \tag{2.13}$$

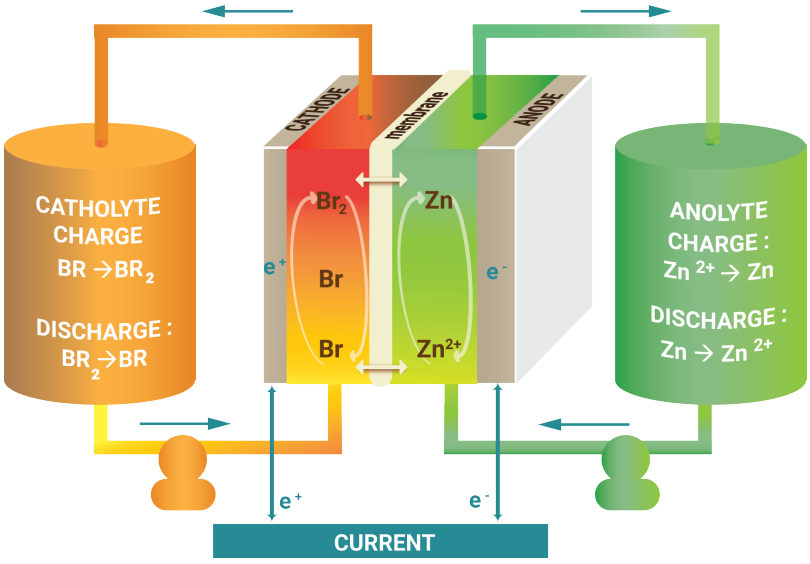

Figure 2.12: Schematic representation of a ZBFB [76]

The state of charge is expressed as the concentration of solid zinc on the electrode surface. Due to the greater cell potential and high density of solid zinc, ZBFB offers higher energy density and power output than VRFB [16]. Zinc is an abundant, recyclable and low cost compound, although bromine gas is corrosive and hazardous, and can cause environmental and public health problems in case of leakage [16].

Sources	Manufacturer	Model	Stack Voltage [V]	Rated Current [A]	Rated Power [kW]	Capacity [kWh]	Electrolyte volume [L]	Discharge time [h]	Efficiency [%]
[77]	Redflow	ZBM2	40-57	60	5	10	100		80
[78]	Primus Power	EnergyPod 2	200-820	225	25	125		5	70

Table 2.5: Technical specifications of commercially available ZBFB [77, 78]

Despite being a relatively new technology, a few commercial options are already available, as shown in Table 2.5. From a comparison between the two options, we can infere that the relation between electrolyte volume and capacity is about 10 L/kWh, and that the discharge time for a 125 kWh battery at rated power of 25 kW is around 5 h.

ZBFB			
V_{cell}	1.85 V	Cell area	200 cm^2
Charge R	0.0001 Ω	Discharge R	0.006 Ω
Charge η	0.08 V	Discharge η	0.1 V
Charge nominal i	0.04 A/cm^2	Discharge nominal i	0.04 A/cm^2
Charge nominal power d.	0.09 W/cm^2	Discharge nominal power d.	0.06 W/cm^2
Depth of discharge	5 - 95 %	Auxiliary losses	6.5 %
Electrolyte max concentration	4 M (Zn), 6 M (Br_2), 3 M ($ZnBr_2$)		

Table 2.6: Summary of model parameters for the ZBFB (validated against experimental data)

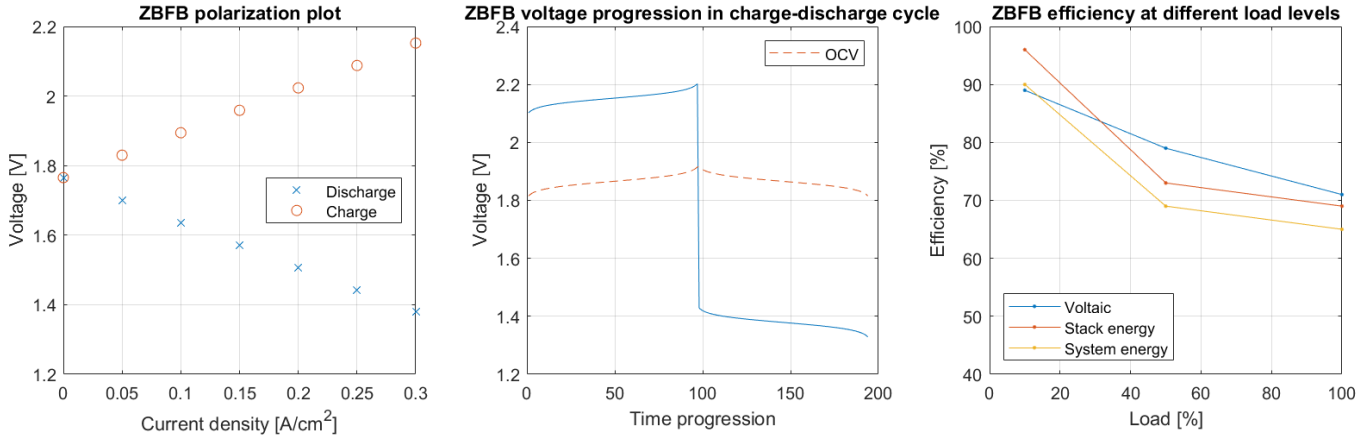

Figure 2.13: Polarization curve (left), voltage progression in charge-discharge cycle (centre), and efficiencies (right) of a ZBFB (validated against experimental data)

Summing up all the information collected from the literature experimental data and

commercial specifications, the ZBFB parameters and behaviour can be modelled as the one showed in Table 2.6 and Figure 2.13.

2.4. Hydrogen system

Although extremely abundant, hydrogen is not considered as a source of energy like fossil fuels. Much of the existing hydrogen is in the form of water and considerable energy is required to extract the desired element. If we take this energy from RES, hydrogen becomes a clean and excellent energy vector for large or small scale storage applications [79].

At present, approximately 96% of all hydrogen used is produced for industrial purposes by chemical means, through the reformation of diverse hydrocarbons, and only 4% is produced by electrolysis of water [79]. Water electrolysis, however, has the potential to become a key element in many sectors for the future sustainable energy system. In recent years, much effort is being put into the research and improvement of water electrolysis to efficiently transform renewable energy in "green" hydrogen [50]. The pure H_2 gas obtained by electrolysis can then be stored and used later to retrieve energy through a fuel cell. In a fuel cell, hydrogen is "combusted" by oxygen, releasing water as the only product. The full Power-to-Power system just described, which in the literature is often referred to as a "Regenerative Fuel Cell" (RFC), can be outlined as in Figure 2.14.

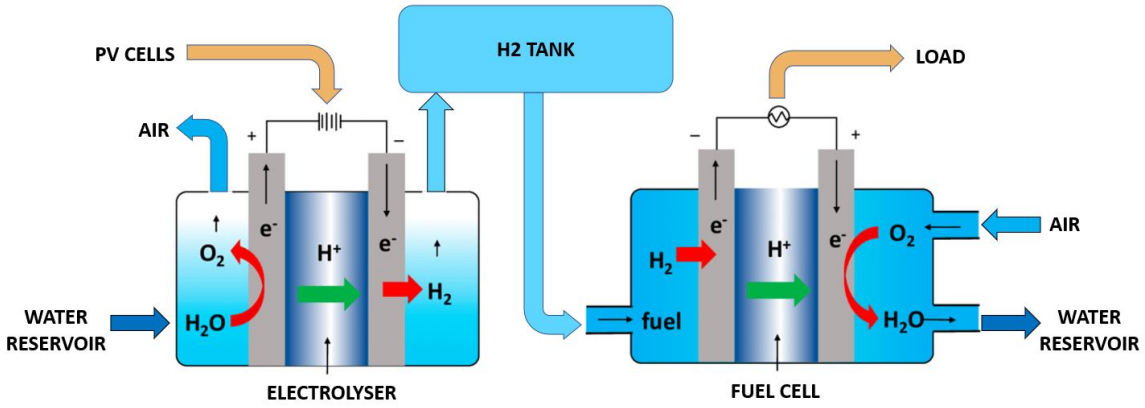

Figure 2.14: Schematic representation of a hydrogen system [80]

A hydrogen storage system is therefore composed by an electrolyser, a fuel cell, a pressurized tank and minor components for auxiliary purposes. The electrolyser and fuel cell can be modelled in a similar way as redox batteries, although, being two separated devices, they can have different sizing. The characteristic reactions and standard potentials in discharge direction (*i.e.* fuel cell) are:

$$\begin{array}{lrcll} \text{Anode:} & 2H^+ + \frac{1}{2}O_2 + 2e^- & \rightarrow & H_2O & V_{an} = 1.23\,V \\ \text{Cathode:} & H_2 & \rightarrow & 2H^+ + 2e^- & V_{cat} = 0.00\,V \\ \text{Overall:} & 2H^+ + \frac{1}{2}O_2 & \rightarrow & H_2O & V_{cell} = 1.23\,V \end{array}$$

The three phases of such a process (hydrogen production, storage and conversion in fuel cells) are described in detail in the next sections.

2.4.1. Hydrogen production

The overall reaction of electrochemical splitting of water into hydrogen and oxygen by supplying electrical energy is given by:

$$H_2O \rightarrow H_2 + \frac{1}{2}O_2 \tag{2.14}$$

At standard conditions, the equilibrium potential for water electrolysis is V_{cell} = 1.23 V. However, at this voltage level the reaction is endothermic and requires additional thermal energy to start. The thermal input can be avoided only above the so called thermoneutral potential, that corresponds to the change in enthalpy for the water splitting reaction and is equal to E^t = 1.48 V. Equilibrium and thermoneutral potential vary with temperature, and some types of electrolysers take advantage of this relation to increase the electrical efficiency.

A basic water electrolysis unit consists of an anode, a cathode, a power supply and an electrolyte. Typically, multiple units are connected in parallel in an electrolyser stack, whose voltage output is the sum of all the single cells output. Direct current is applied at the extremes and electrons flow from anode to cathode, while ions are transferred through the electrolyte solution to keep the electrical charge in balance [81]. To improve the ionic conductivity, compounds that readily dissociate to form ions in water (typically acids or bases) are added to the electrolyte. Electrolysers are therefore classified according to the electrolyte used, and the main three types are alkaline (AEL), polymer electrolyte membrane (PEMEL) and solid oxide (SOEL) [82]:

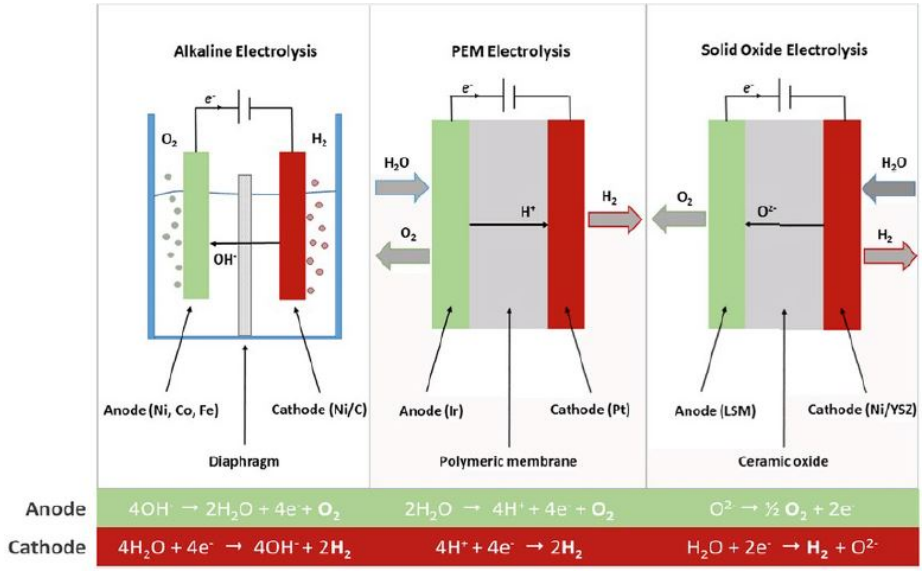

Figure 2.15: Schematic representation of electrolyser types and half-reactions [83]

- In AEL, electrodes are immersed in a KOH basic solution and separated by a diaphragm. It is the most mature and less expensive technology.
- In PEMEL, the electrolyte is acidic and a proton exchange membrane (usually Nafion®) separates the half-cells. The corrosive acidic environment requires the use of noble metals as catalysts (iridium for anode, platinum for cathode), increasing the price.
- In SOEL, the electrolyte dissociates in oxygen ions that permeate through a ceramic insulating layer. They operate at very high temperature, achieving higher efficiencies but requiring external heating and attention to material stability.

An overview of the characteristics of each type is given in Table 2.7.

Parameter	**AEL**	**PEMEL**	**SOEL**
Operating temperature [°C]	60-80	50-80	700-900
Operating pressure [bar]	10-30	20-50	1-15
Current density [A/cm^2]	0.25-0.45	1.0-2.0	0.3-1.0
Cell voltage [V]	1.8-2.4	1.8-2.2	0.7-1.5
Voltage efficiency [$\%_{HHV}$]	62-82	67-82	< 100
Start-up time	1-5 min	< 10 s	15 min
System response	sec	msec	sec
Lifetime [10^3 h]	60-90	20-60	< 10
Investment cost [€/kW]	1000-1200	1860-2320	> 2000

Table 2.7: Comparison of the technical characteristics of different electrolyte types [82, 84]

High temperature electrolysis (SOEL) is a relatively new technology and, despite its higher efficiency, has several shortcomings which make it the less suitable for our purpose. On the other hand, both low temperature technologies have similar and promising features. AEL offers the advantage of simplicity, technical maturity, durability and lower costs [81], but is also less powerful and responsive than PEMEL. Despite the higher cost, PEM electrolysers prove to be the most suitable for this kind of application.

Buttler and Spliethoff [82] recently published a review of the current status of electrolysis for energy storage. According to their findings, PEM electrolysers are typically operated at current densities up to 2 A/cm^2 and pressures up to 35 bar, and their performance can be summarized as follows:

- At nominal current (2 A/cm^2) the energy consumption is about 5 kWh/Nm$^3_{H2}$, corresponding to an efficiency of 60% with respect to the LHV of hydrogen (equal to 3.00 kWh/Nm$^3_{H2}$)

- At part-load operation (0.1 A/cm^2) the energy consumption decreases to 3.8 kWh/Nm$^3_{H2}$, correnspondig to an efficiency of 79%
- The overall system consumption, including auxiliary devices, is about 5.25 kWh/Nm$^3_{H2}$, corresponding to an overall efficiency of 57%

The performance values just mentioned agree with the technical specifications of commercially available electrolysers listed in Table 2.8.

Souces	Manufacturer	Model	Max pressure [bar]	H_2 production [Nm^3/h]	Power cons. [kW]	Energy cons. [kWh/Nm^{3}3]	Efficiency wrt LHV [%]
[85]	Angstrom Adv.	HGHI70000	4	10	60	5.8	52
[86]	Areva H2Gen	E5 - E120	35	5 - 120	40 - 960	4.8 - 5.7	68
[87]	Giner Inc	Allagash	40	400	2000	5	60
[88]	GreenHydrogen	HyProvide P1	50	1	10	5.5	55
[89]	Hydrogenics	HyLYZER - 3000	30	300	1500	5 - 5.4	56 - 60
[90]	ITM Power	HGAS1SP - 3SP	20	125 - 409	700 - 2350	5.6 - 5.7	54
[91]	Kobelco Eco-Sol.	SH/SL60D	4 - 8	10	60	5-5 - 6.5	46 - 55
[92]	NelHydrogen	C10 - C30	14 - 30	10 - 30		5.8 - 6.2	48 - 52
[93]	McPhy	McLyzer Small	30	10 - 20	50 - 100	4.5	67
[94]	Proton On Site	M100 - M400	30	104 - 414	510 - 2100	4.9 - 5.1	60
[95]	Pure Energy C.		30	2.7 - 42.6	15 - 230	5.4 - 5.7	
[96]	Siemens	Silyzer 300	35	3860	17500	4.5	67
[97]	Suzhou Jingli	DQ 100	32	100			
[98]	Taledyne En. Sys.	Titan HMXT	10	2.8 - 11.2		4.8	63
[99]	Treadwell Corp.		76	10.2			

Table 2.8: Technical specifications of commercially available electrolysers [85–99]

2.4.2. Fuel cells

Fuel cells physics, structure and types are similar to the ones of electrolysers, since they perform the same chemical reaction but in opposite directions.

The overall reaction of water recombination in a fuel cell is:

$$2H_2 + O_2 \rightarrow 2H_2O \tag{2.15}$$

The electrons produced at the anode and collected at the cathode pass through an external circuit, where the electron flow is captured by a generator. Due to the activation energy and voltage losses explained before, the actual voltage that one cell is able to develop is only around 0.7 V. For this reason, to reach a useful output voltage, multiple cells are connected in series in a compact design characterized by "bipolar plates": electrically conductive plates that act as both anode and cathode

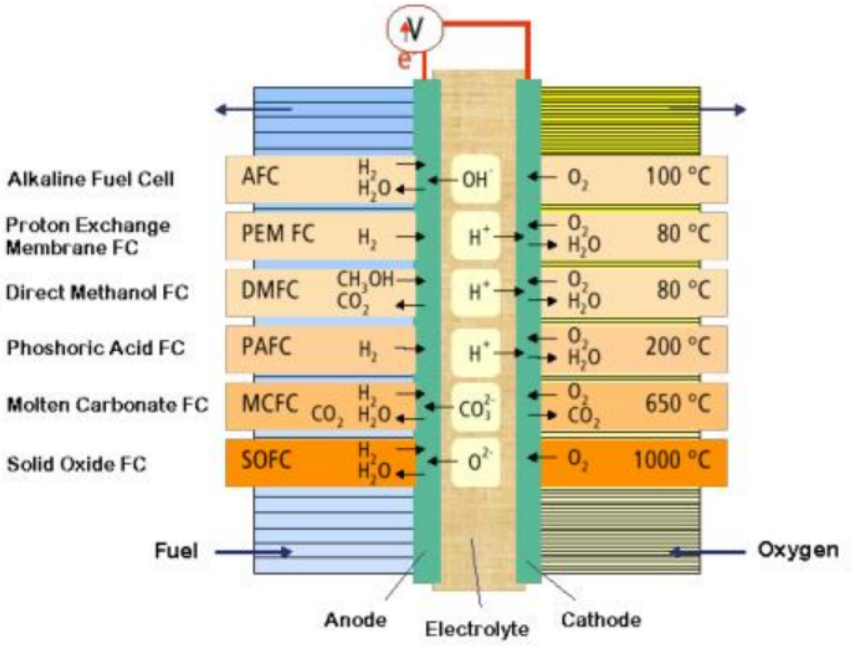

Figure 2.16: Schematic representation of fuel cell types and half-reactions [83]

of two adjacent cells, and have vertical and horizontal channels to let the reactant gases flow [100].
As for electrolysers, different types of fuel cells exist depending on the electrolyte used: alkaline (AFC), polymer electrolyte membrane (PEMFC), direct methanol (DMFC), phosphoric acid (PAFC), molten carbonate (MCFC) and solid oxide (SOFC). Some of them require the presence of carbon compounds in the fuel mixture (methanol for DMFC and CO_2 for MCFC), consequently they emit carbon dioxide. They are shown in Figure 2.16 alongside with their electrolyte ion, reactants, products and optimal operating temperature.

Parameter	**PEMFC**	**AFC**	**PAFC**	**SOFC**
Operating temperature [°C]	60-80	60-90	200	900-1000
Operating pressure [bar]	1-3	1-5	1-8	1-10
Current density [A/cm^2]	< 1	0.1-0.2	< 0.8	< 1
Electrical efficiency [%]	40-50	> 60	40-55	60
Start-up time	< 1 min	mins	1-3 h	hours
Load flexibility	fast	fast	very fast	slow
Lifetime [$10^3 h$]	2-4	5	> 40	> 30
Investment cost [€/kW]	2000	1200	2400	2150

Table 2.9: Comparison of the technical characteristics of different fuel cell types [101–103]

PEMFC, AFC and SOFC have the same working principles as their correspondent

electrolyser. DMFC and MCFC are not considered in this analysis as they cannot be considered a fully carbon-free technology. A similar analysis as for electrolyser types is provided for the remaining technologies in Table 2.9.

Similarly in this case, a clear distinction between high and low temperature fuel cells in present. Despite the higher efficiency and current density due to the high temperature, PEMFC has better start-up time and load flexibility, which are the most relevant parameter for our purpose. Therefore, it appears the most suitable type for small-scale storage application.

Hydrogen fuel cells are extensively studied as engines for cars, ships or airplanes, while their stationary application is less investigated in the literature. However, there are some commercial options for this kind of application:

Sources	Manufacturer	Model	Voltage [V]	Nominal current [A]	Nominal power [kW]	H2 consumption rate [L/min]
[104]	Ballard	FCgen - HPS	202	645	140	
[104]	Ballard	FCgen - LCS	176	360	2.3 - 63.4	
[105]	Elring Klinger	EKPO NM5-EVO	201	380	76	
[105]	Elring Klinger	NM12 Single	215	570	123	
[105]	Elring Klinger	NM12 Twin	359	570	205	
[106]	Horizon	VL30 - VL100	100 - 180	270	33	
[106]	Horizon	H12 - H5000	7.8 - 72	1.5 - 70	0.012 - 5	0.18 - 65
[107]	Nedstack	FCS 7-XXL	46.6 - 29.5	230	6.8	77
[107]	Nedstack	FCS 10-XXL	46.1 - 72.8	230	10.6	572
[107]	Nedstack	FCS 13-XXL	58.9 - 93.2	230	13.6	732
[108]	PlugPower	GenSureHP	480		250 - 1000	
[108]	PlugPower	ReliOn E-1000x	48 - 24	21 - 42	1	
[108]	PlugPower	ReliOn E-2200x	48 - 24	46.5 - 93	2.2	

Table 2.10: Technical specifications of commercially available fuel cells [104–108]

2.4.3. Hydrogen storage

Hydrogen is the element with lowest volumetric density, which is a major issue for storage. In order to increase the hydrogen density in a storage system, either work must be performed to compress hydrogen, or temperature has to be decreased below the critical temperature or finally, the repulsion between hydrogen molecules (or atoms) has to be reduced through interaction of hydrogen with another material. An important criteria for hydrogen storage is the reversibility of the uptake and release.

There are several methods to reversibly store hydrogen with an increased volumetric and gravimetric density. The most relevant ones are the following:

- *Compressed gas* is the most commonly used and commercialized storage method for gaseous fuels. High pressure gas cylinders with a maximum pressure of 20 MPa are commonly used as tank, but new lightweight composite cylinders have been developed, which are able to withstand a pressure up to 80 MPa, reaching a hydrogen volumetric density of 36 kg/m^3 [109]. The major drawback is the relatively small amount of hydrogen that may be stored in a reasonable volume. The efficiency of energy storage by compressed hydrogen gas is about 94% [110].

- *Liquid hydrogen* is stored at ambient pressure in cryogenic tanks at 21.2 K. The challenges of liquid hydrogen storage are energy efficient liquefaction and thermal insulation of the cryogenic storage vessel to reduce boil-off of hydrogen, due to its low critical temperature (33K). The large amount of energy necessary for the liquefaction and the boil-off limit the possible applications to niches where cost is not an important issue and hydrogen is consumed in a rather short time [109].

- *Physisorption* is the adsorption of gas on a solid surface as a consequence of the field force at the surface of the adsorbent, which attracts the molecules of the gas or vapor. The amount of hydrogen that can be adsorbed is proportional to the specific surface area of the adsorption substrates. The most popular adsorbent materials are activated carbon, with a hydrogen adsorption capacity of 0.0015 $mass\%m^{-2}g$ at 77 K, and carbon nanotubes. It is a promising technology for mobile application as adsorbent materials are lightweight, however it is still very expensive [110].

- *Metal hydride storage* is relatively new compared with pressure vessel and liquid hydrogen. In metal hydride storage, hydrogen molecules are chemically bonded with metals or alloys. Heat is generated during hydrogen charging (absorption) and the same heat is needed to discharge the hydrogen (desorption). Metal hydride storage may be a suitable and affordable option when weight is not a major concern due to the heavy metals or alloys. However, speed of charging/discharging and stability under frequent cycles should be improved [110].

An overview of the densities and operational parameters of these technologies is given in Table 2.11.

At the moment, despite its low volumetric density, compressed gas in pressure vessels is the most favorable technology because of its maturity, simplicity, high storage energy efficiency and low cost. This storage method seems the most suitable one for a residential application, in which energy efficiency is important and space is not a major constraint.

2.4.4. Overall system

Putting together all the information from the literature and commercial options, the resulting parameters and behaviour of a complete hydrogen system is showed in

Storage method	Volumetric density [kgH_2/m^3]	Gravimetric density [$mass\%$]	Pressure [bar]	Temperature [K]
Compressed gas	< 36	13	800	298 (standard)
Liquid hydrogen	71	100	1 (standard)	21
Physisorption	20	4	70	65
Metal hydrides	< 150	2	1 (standard)	298 (standard)

Table 2.11: Overview of technical characteristics of different hydrogen storage technologies [109]

Table 2.12 and Figure 2.17

Hydrogen system			
V_{cell}	1.23 V	Cell area	100 cm^2
Charge R	0.24 Ω	Discharge R	0.24 Ω
Charge and discharge i	$\frac{RT}{2F}(arcsinh(\frac{i}{2\cdot1.65\cdot10^{-8}}) + arcsinh(\frac{i}{2\cdot0.09}))$		
Charge nominal i	2 A/cm^2	Discharge nominal i	1.2 A/cm^2
Charge nominal power d.	3.9 W/cm^2	Discharge nominal power d.	0.84 W/cm^2
Depth of discharge	0 - 100 %	Auxiliary losses	7 % (EL), 10 % (FC)
Electrolyte max concentration	100 bar H_2		

Table 2.12: Summary of model parameters for a hydrogen system (validated against experimental data)

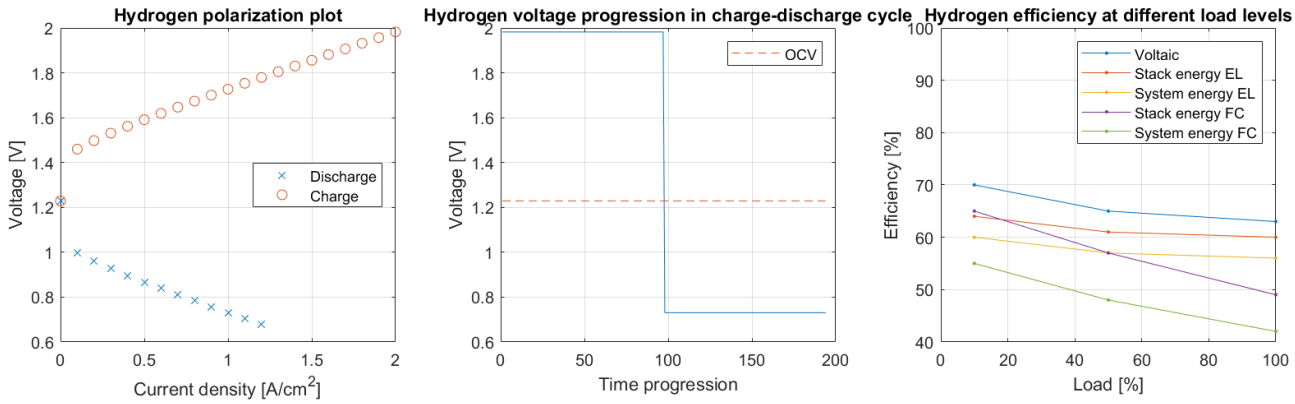

Figure 2.17: Polarization curve (left), voltage progression in charge-discharge cycle (centre), and efficiencies (right) of a hydrogen system (validated against experimental data)

3 Optimization

In order to determine the economic feasibility of a system, a model was built in GAMS, an optimization and modelling software. The purpose of the model is to find the optimal size of the PV system and of the battery such that the system cost, spread over the whole lifetime of the project, is minimized.

An optimization is made op of an objective function, some variables, some parameters and some constraints. In the following sections, all these different components are described and explained.

3.1. Variables

3.1.1. Photovoltaic variables

Power P_{PV} generated by photovoltaic panels is

$$P_{\text{PV}} = \eta(t) G(t) A \tag{3.1}$$

The first two factors $\eta(t)$ and $G(t)$ depend on climate, while the panel area A identifies the size of the system. PV panels have now an efficiency close to 20% and in the future this efficiency is estimated to reach 30% [111]. This is accounted for in the optimization through a multiplicative factor only inserted in the future case, calculated as 30/19.2 = 1.5625.

3.1.2. Storage variables

The storage devices analysed in this studies (flow batteries and electrolyser/fuel cell system) have the peculiarity of allowing independent power and energy scaling, therefore these two sizes are optimized separately.

Power P_{S} stored and delivered by an electrochemical storage device scales with the number of cells (N) present in the system. Its value is limited by the characteristic cell voltage, which for many batteries depends on the state of charge (SOC), and by the maximum charge or discharge current density. For this model, a polynomial expression for the maximum cell power $P_{cell,\text{MAX}}$ as function of the SOC is derived for each storage technology:

$$\begin{aligned} P_{\text{S}} &\leq N P_{\text{cell,MAX}}(\text{SOC}) \\ P_{\text{cell,MAX}}(\text{SOC}) &= \alpha \cdot \text{SOC} + \beta \end{aligned} \tag{3.2}$$

	Charge		Discharge	
Storage technology	α	β	α	β
VRFB	0.7991	354.28	0.6712	214.64
HBFB	0.1512	129.52	0.1512	44.52
ZBFB	0.0454	126.87	0.0454	80.43
Hydrogen	0[1]	387.78	0[1]	80.59

Table 3.1: Polynomial coefficients for $P_{\text{cell,MAX}}$ calculation as function of SOC (own model validated against experimental data)

The sizing variable for the optimization is the number of cells N.

The energy storage capacity lies in the volume of electrolyte or gas that can be accumulated. Assuming a constant charging and discharging energy efficiency ϵ, that accounts for all the stack and system losses, the energy content of the battery is calculated at each new timestep depending on how much power is stored or delivered in the previous timestep:

$$E_{\text{S}}(t+1) = E_{\text{S}}(t) + P_{\text{S,c}}(t)\Delta t \cdot \epsilon_{\text{c}} - \frac{P_{\text{S,d}}(t)\Delta t}{\epsilon_{\text{d}}} \tag{3.3}$$

	Storage technology	ϵ_{c}	ϵ_{d}
PRESENT	VRFB	86%	86%
	HBFB	85%	82%
	ZRFB	86%	86%
	Hydrogen	70%	60%
FUTURE	VRFB	88%	88%
	HBFB	85%	82%
	ZBFB	88%	88%
	Hydrogen	84%	70%

Table 3.2: Present and future energy storage efficiencies for energy capacity calculation of each storage technology (own model validated against experimental data)

The total energy capacity $E_{\text{S,tot}}$ is then determined through the SOC definition and boundaries:

$$\begin{aligned} \text{SOC}(t) &= \frac{E_{\text{S}}(t)}{E_{\text{S,tot}}} \\ 0 \leq \text{SOC}(t) &\leq 1 \quad \forall t \in \{\text{year}\} \end{aligned} \tag{3.4}$$

[1] $P_{\text{cell,MAX}}$ for hydrogen production and oxidation is not SOC-dependent

3.1.3. Grid variables

At each timestep, the remaining power required to balance the system is bought or sent back to the main grid. The grid is a "passive" component, whose size is simply defined as the amount of energy bought $E_{\text{G,i}}$ or sold back $E_{\text{G,o}}$, calculated as:

$$E_{\text{G,i}} = \sum_{t}^{\text{year}} P_{\text{G,i}}(t)\Delta t$$
$$E_{\text{G,o}} = \sum_{t}^{\text{year}} P_{\text{G,o}}(t)\Delta t \tag{3.5}$$

In conclusion, the 5 variables representing the power sources are:

$$A, \quad N, \quad E_{\text{S,tot}}, \quad E_{\text{G,i}}, \quad E_{\text{G,o}}$$

representing the PV panel area A [m^2], the number of storage cells N, the total storage energy capacity $E_{\text{S,tot}}$ [kWh], the energy bought from the grid $E_{\text{G,i}}$ [kWh] and the energy sold to the grid $E_{\text{G,o}}$ [kWh].

3.2. Objective function

The economic feasibility of the different storage technologies is investigated through a sizing optimization based on costs. Specifically, the size of the residential PV-storage system components that yield to the minimum total cost of energy is evaluated for a minimum level self-consumption.

As explained in Chapter 4, the levelized cost of energy (LCOE) formula is used to evaluate the economic viability of our system. The total LCOE of the system including load, PV panels, a storage system and grid connection can be written as:

$$\text{LCOE} = \frac{(Cost_{\text{PV}} + Cost_{\text{S}} + Cost_{\text{G}})}{E_{\text{L}} F} \tag{3.6}$$

This equation is the objective function to be minimized in order to obtain the optimal solution. The cost of every component depends on the corresponding variables representing their size and nominal power or energy:

$$Cost_{\text{PV}} = (In_{\text{PV}} \cdot A)(1 + Op_{\text{PV}} F) \tag{3.7}$$
$$Cost_{\text{S}} = (In_{\text{S,fix}} + In_{\text{S,membr}} \cdot NS_{\text{cell}} + In_{\text{S,power}} \cdot NP_{\text{cell,MAX}} + In_{\text{S,energy}} \cdot E_{\text{S,tot}})(1 + Op_{\text{S}} F) \tag{3.8}$$
$$Cost_{\text{G}} = In_{\text{G}} + Op_{\text{G,i}} F \cdot E_{\text{G,i}} + In_{\text{G,o}} + Op_{\text{G,o}} F \cdot E_{\text{G,o}} \tag{3.9}$$

The numerical value corresponding to each cost item is detailed in Chapter 4.

3.3. Constraints

In order to accurately describe the system, the following constraints are used.

Storage:

$$\begin{aligned} &\text{if} \quad P_{\mathsf{L}}(t) \geq P_{\mathsf{PV}}(t) \quad \text{then} \quad U(t) = 1 \\ &\text{if} \quad P_{\mathsf{L}}(t) < P_{\mathsf{PV}}(t) \quad \text{then} \quad U(t) = 0 \end{aligned} \tag{3.10}$$

$$P_{\mathsf{S,d}}(t) \leq NP_{\mathsf{d,MAX}}(\mathsf{SOC}, t) \cdot U(t)$$

$$P_{\mathsf{S,c}}(t) \leq NP^{t}_{\mathsf{c,MAX}}(\mathsf{SOC}, t) \cdot (1 - U(t)) \tag{3.11}$$

Equations 3.11 make use of the binary variable U to avoid simultaneous charging and discharging. The variable is defined according to the sign of current mismatch ($P_{\mathsf{L}} - P_{\mathsf{PV}}$) through conditional statements in 3.10.

Balance:

$$\begin{aligned} P_{\mathsf{PV}}(t) &= P_{\mathsf{P,L}}(t) + P_{\mathsf{S,c}}(t) + P_{\mathsf{G,o}}(t) \\ P_{\mathsf{L}}(t) &= P_{\mathsf{P,L}}(t) + P_{\mathsf{S,d}}(t) + P_{\mathsf{G,i}}(t) \\ P_{\mathsf{PV}}(t) - P_{\mathsf{L}}(t) + P_{\mathsf{S,d}}(t) - P_{\mathsf{S,c}}(t) + P_{\mathsf{G,i}}(t) - P_{\mathsf{G,o}}(t) &= 0 \end{aligned} \tag{3.12}$$

Photovoltaic power usage, load share and the whole system are balanced at every timestep through constraints 3.12.

self-consumption:

$$1 - \frac{E_{\mathsf{G,i}}}{E_{\mathsf{L}}} \geq \mathsf{SC} \tag{3.13}$$

The self-consumption (SC) of the system is defined as the amount of load consumption met by energy produced by internal devices (PV and storage). For convenience, in this model it is calculated as the reciprocal of the load consumption satisfied by the grid. Constraint 3.13 sets the minimum self-consumption at a predefined value indicated with SS (in the 50% - 100% range).

4
Costs

4.1. Levelized Cost of Energy

One of the most used methods to investigate the economic viability of distributed generation projects is evaluating the levelized cost of energy (LCOE) [112]. It essentially represents the lifecycle cost divided by the lifetime energy production of a component in an energy system, and it aims at comparing different technologies in terms of their capital, operation, maintenance costs and performance. The formula for each power unit can be written as:

$$\text{LCOE} = \frac{In_0 + \sum_{t=1}^{L} \frac{Fuel_t + Op_t}{(1+r)^t}}{\sum_{t=1}^{L} \frac{E_t}{(1+r)^t}} \tag{4.1}$$

where t represents time in years, L is the project lifetime, In_0 is the investment cost incurring all at time 0, $Fuel_t$ are fuel costs and Op_t are operation and maintenance costs in the year t, and E_t is the total energy provided by that component in the year t.

The $(1+r)^t$ factor accounts for the compound interest in time, where r represents the annual discount rate or weighted cost of capital (), which is a fundamental driver in investment decisions. Studies show that the WACC varies between technologies, countries and over time as technologies mature [113], influencing the model outcome. For this study, r is taken as 4% for Netherlands and 5% for Italy as calculated in [113]. For the sake of simplicity, in the model the discount rate is approximated as:

$$\sum_{t=1}^{L} \frac{1}{(1+r)^t} \approx \frac{1-(1+r)^{-L}}{r} = D \tag{4.2}$$

Therefore, the total LCOE of a system including load, PV panels, a storage system and a grid connection (all with zero fuel consumption) can be written as:

$$\text{LCOE} = \frac{In_{\text{PV}} + Op_{\text{PV}}D + In_{\text{S}} + Op_{\text{S}}D + In_{\text{G}} + Op_{\text{G}}D}{E_{\text{L}}D} \tag{4.3}$$

The total energy generated by all the power units equal to the energy consumed by the load, therefore E_{L} is taken as the yearly electricity consumption of the reference house in kWh.

Investment and maintenance costs are different for each component and depend on several factors, like rated power or physical size. In the next sections an analysis of the current and future costs is presented.

4.2. Photovoltaic cost

According to IRENA, the cost of crystalline solar PV modules declined by around 90% between 2009 and 2019, becoming increasingly competitive with the electricity prices on the market [114], and will continue to decrease.

Investment costs related to PV can be subdivided into three main categories:

- Hard costs related to hardware costs of every piece of material needed to build the system
- Installation costs related to the setup of the PV system
- Soft costs comprising permits, marketing, sales and administrative costs associated with the system

Accepting the assumption that there is a common EU market, the hardware cost is considered constant among countries. The reference used here is for crystalline-Silicon fixed-axis panels produced in Germany [115]. On the other hand, soft and installation costs are more heterogeneous and depend on average worker wages. Maintenance costs can be taken as 1% of the total investment costs for fixed-angle configurations [115]. In the future, according to an analysis performed by the Fraunhofer ISE institute [111] based on the current scenario and the photovoltaic learning curve, prices will halve with respect to current ones and module efficiency will reach 30% on average.

Following these considerations, the current and future prices for Netherlands and Italy, converted to €/m^2 (1 kWp = ca. 5 m^2) are shown in Table 4.1.

	Location	In_{PV}	Op_{PV}
		€/m^2	€/m^2 year
PRESENT	Rotterdam	163.95	1.64
	Palermo	136.99	1.37
FUTURE	Rotterdam	86.40	0.86
	Palermo	76.80	0.77

Table 4.1: Summary of photovoltaic costs [111, 115]

4.3. Storage cost

Electricity storage is currently an economic solution off-grid, in solar home systems and mini-grids where it can increase the fraction of renewable energy, as well as in the case of islands or other isolated grids [28]. Emerging market segments include the pairing of storage with residential rooftop solar PV to increase self-consumption and/or to avoid peak demand charges by levelling load.

Flow batteries and hydrogen systems are still developing and not broadly commercialized, therefore their cost assessment is afflicted with uncertainties. Nevertheless, thanks to techno-economic analysis and economic models found in literature, it is possible to roughly estimate their cost. Missing or unclear data was deduced from generic cost estimations, sometimes taking advantage of the similarities between the different technologies. In the following section, the resulting costs for each storage technology are outlined.

4.3.1. Redox-flow batteries cost

Estimating the commercial present and future cost of a redox-flow battery is not an easy task, as it includes a set of developing technologies that have been tested and analysed for different applications in a wide range of power and energy capacities.

The total investment cost for a RFB is usually calculated as follows:

$$I_{\text{S}} = Cost_{\text{area}} \cdot NA + Cost_{\text{power}} \cdot NP_{\text{cell,MAX}} + Cost_{\text{energy}} \cdot E_{\text{S}} \tag{4.4}$$

where the cost components are defined as:

- Cost of area $Cost_{\text{area}}$ [€/m^2], related to stack components (membranes, electrodes, bipolar plates, current collectors, end plates, catalysts)
- Cost of power $Cost_{\text{power}}$ [€/kW], related to the inverter, power conversion system (PCS) and balance of plant (BOP) components
- Cost of energy $Cost_{\text{energy}}$ [€/kWh], related to the electrolyte chemicals, tanks and flow management devices (pipes, pumps, valves)

Maintenance and operation costs are usually expressed as a percentage of the investment costs.

Minke and Turek [116] recently reviewed all the available literature on techno-economic assessment of vanadium batteries, and found that the significant differences in system boundaries and input data result in a wide range of VRFB costs (564-12931 €/kW or 89–1738 €/kWh). The main reference for this work is Noack et al.'s techno-economic model of a 10 kW, 120 kWh vanadium battery [117], that provides a detailed cost breakdown of all the device components.

On the other hand, only two economic studies are found regarding the hydrogen-bromide RFB [73, 118], among which Hugo et al.'s paper [73] provides a useful cost breakdown of the HBFB system.

Despite being a more developed technology, few papers are found about economic models of zinc-bromine batteries. Cost data for this battery type was mainly taken from a recent PhD thesis by Hao Xin [119] and validated against IRENA's findings [28].

Estimated present costs of each cost category are summed up in Table 4.2 and can be explained as follows:

- The cost for a standard Nafion™ion exchange membrane for present day scenarios is 230 €/m^2 on average. Other stack components have similar costs for the VRFB and HBFB, resulting in a total stack cost of around 1200 €/m^2, including assembly.
- Current collectors and end plates are estimated at 100 €/kW for VRFB and HBFB and at 45 €/kW for ZBFB. The bidirectional inverter can be assumed equal for all battery types, costing around 145 €/kW. Another 100 €/kW is allocated for control and BOP devices.
- Electrolytes, tanks and flow management costs are the ones varying more between different technologies. Vanadium is relatively expensive (8-22 €/kg) but doesn't require a cooling system, which is instead necessary for HBFB. Zinc bromide and bromine are less expensive (0.33 $/kg and 0.63 $/kg respectively [120]), but their higher specific energy leads to a relatively large cost. System assembly costs are also considered here.

	Battery type	In_{S}			Op_{S}
		$Cost_{\text{area}}$	$Cost_{\text{power}}$	$Cost_{\text{energy}}$	
		€/m^2	€/kW	€/kWh	€/year
PRESENT	VRFB	1280	365	450	1.5 %
	HBFB	1163	365	350	1.5 %
	ZBFB	1200	290	480	1.5 %
FUTURE	VRFB	120	100	100	1.0 %
	HBFB	324	245	134	1.0 %
	ZBFB	150	157	144	1.0 %

Table 4.2: Summary of redox-flow batteries costs [28, 73, 116–119]

Costs for the future scenario have been estimated from component price drop previsions and from overall system price reduction projections. VRFB and ZBFB are projected to reduce their price by 66% in the future according to IRENA [28], while HBFB is estimated to reach the cost of 128 €/kWh [73].

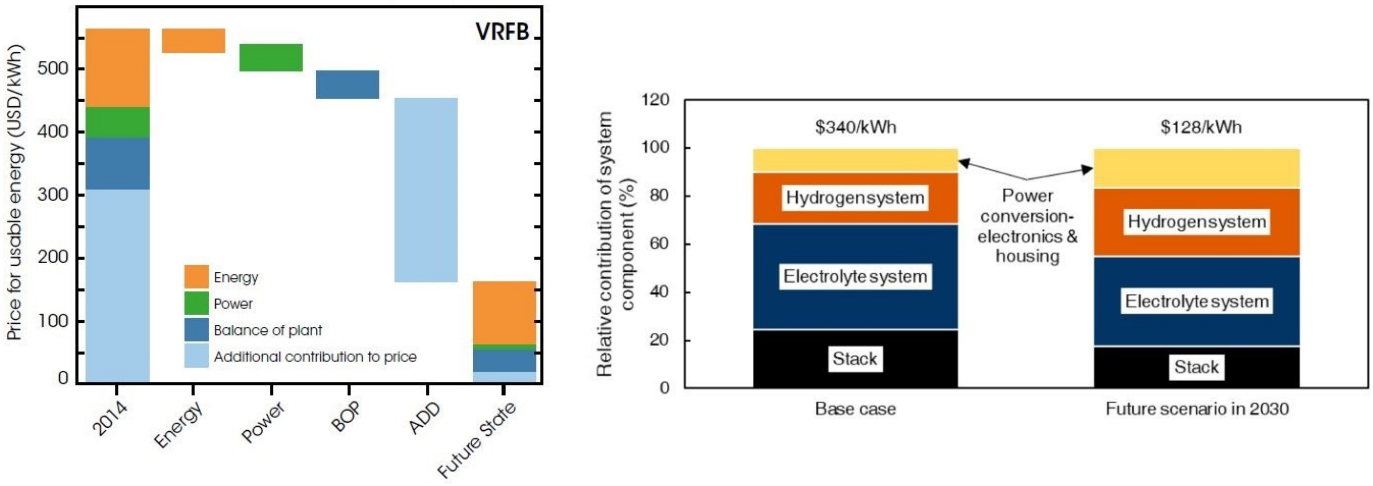

Figure 4.1: Cost reduction pathway from present to future scenario for VRFB (left) and HBFB (right)

4.3.2. Hydrogen system cost

As previously explained, an hydrogen storage system has separate charging and discharging components, the electrolyzer and the fuel cell respectively. A storage tank is also necessary in order to stock fuel. Therefore, the total investment cost for such a system are given as:

$$In_{\mathrm{S}} = Cost_{\mathrm{EL}} \cdot N_{EL} P^{EL}_{\mathrm{cell,MAX}} + Cost_{\mathrm{FC}} \cdot N_{FC} P^{FC}_{\mathrm{cell,MAX}} + Cost_{\mathrm{tank}} \cdot E_{\mathrm{S}} \tag{4.5}$$

where the coefficients are defined as follows, and the corresponding numerical values are collected in Table 4.3:

- Cost of electrolyzer $Cost_{\mathrm{EL}}$ [€/kW], related to a PEM device. In the present, the expense results to be 957 €/kW, whereas forecasts for future scenarios indicate a decrease up to 305 €/kW [121].
- Cost of fuel cell $Cost_{\mathrm{FC}}$ [€/kW] of PEM type. Despite the prevalence of fuel cell manufacture for automobile applications, a current cost of 2500 €/kW can be estimated for stationary applications [122], with a projected future cost drop to of 325 €/kW [123].
- Cost of storage $Cost_{\mathrm{tank}}$ [€/kWh] related to the H_2 tank, BOP components and all storage-related devices. For this project, a Type IV low pressure vessel is employed. The considered costs are extracted from James et al. [124]: the current cost is 23 €/kWh while in the long-term period, with increasing manufacturing expertise, the cost is expected to drop to 10 €/kWh.

Maintenance and operation costs Op_{S} are taken as 2 % of the total investment costs [125] and assumed to halve in the future.

	In_S			Op_S
	C_{EL}	C_{FC}	C_{tank}	
	€/kW	€/kW	€/kWh	€/year
PRESENT	957	2500	23	2.0%
FUTURE	305	325	10	1.0%

Table 4.3: Summary of hydrogen system costs [121–124]

4.4. Grid cost

The operational cost of the grid component in the present system is nothing else than the cost of buying energy from the DSO. Electricity market prices depend on a range of different supply and demand conditions, including the geopolitical situation, the national energy mix, import diversification, network costs and taxation, and are therefore different for each country. For this work, they are taken from recent statistics as 0.1361 €/kWh in the Netherlands and 0.2153 €/kWh in Italy [126].

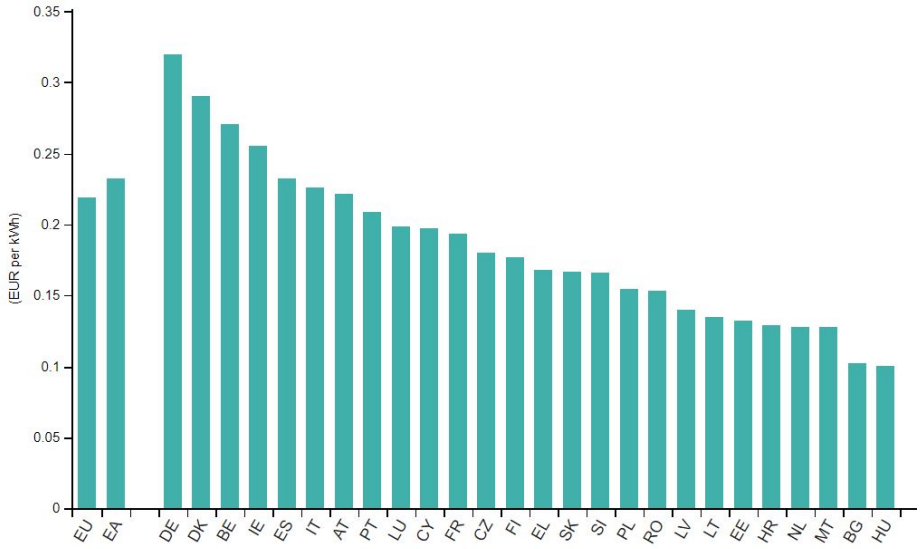

Figure 4.2: Price of electricity in European countries in 2021 [126]

The main drivers influencing the electricity prices in the future are fossil fuel prices, CO_2 prices, the levels of the electricity demand, the decommissioning of the existing capacity (e.g nuclear) and the deployment of renewable energy [127]. Several models can be made to estimate future electricity prices, for this work it is assumed that the increase in CO_2 prices and of investments in renewable energies will determine an increase of 50% with respect to current prices [128].

Investment costs are represented by the cost of grid connection, which is assumed at 50 €/kW [129], i.e. 150 € for a household with 3 kW of maximum power.

	Location	In_{G}	Op_{G}
		€/kW	€/kWh
PRESENT	Rotterdam	50	0.1361
	Palermo	50	0.2153
FUTURE	Rotterdam	50	0.2042
	Palermo	50	0.3230

Table 4.4: Summary of grid costs [126, 128, 129]

5 Results

5.1. Outline of results

Chapter 5 collects the outputs of the optimization process. Several simulations have been performed in order to study the feasibility of the different technologies in the various situations. The diagram in Figure 5.1 tries to summarise the studied cases.

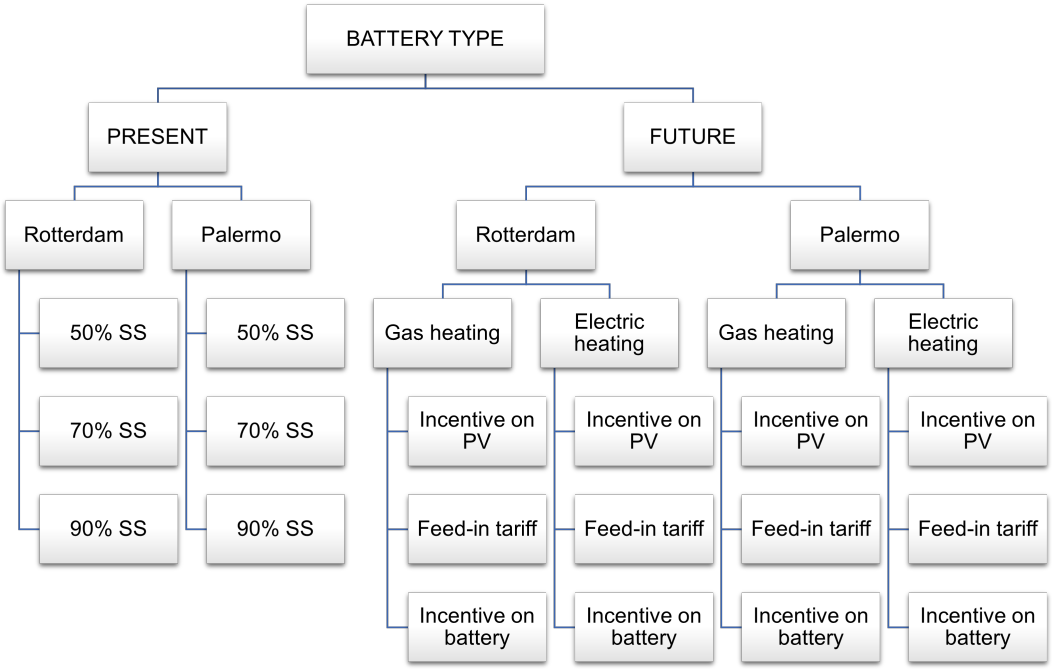

Figure 5.1: Scheme of the optimization scenarios considered

For each technology, the present scenario is first investigated. The behaviour of the systems in the two sites, Rotterdam and Palermo, was simulated at different levels of self-consumption. The three percentages of autonomy allow to study the LCOE dependency on self-consumption.

Available estimates on projected scenarios give the possibility of investigating future applications of the considered storage systems. Since in the next years the load consumption is likely to change, the two diverse load conditions (gas and electric heating) are studied. It stands to reason that in the future there might be greater

incentives to promote renewable energy utilization, therefore three different kinds of subsidies are hypothesized and implemented in the simulations:

- **Incentive on PV** which is the same bonus adopted in the present case, i.e. 50% incentive over the PV investment cost.
- **Feed-in tariff** which is not a one-time incentive, but rather a policy mechanism that provides compensation to the prosumer when he enters power into the grid. 50% of the projected grid energy cost was taken as revenue for the electricity given back.
- **Incentive on battery** which corresponds to a 50% discount over the storage system capital expense.

5.2. Example of system behaviour

As explained in Chapter 3, the model's purpose is to find the optimal sizing of the system components such that the cost is minimized. In doing this, the software also identifies the optimal control strategy, modulating the power flow from and to the different components. In this sense, the LCOE obtained from the optimization is only ideal, as in the real case it is not possible to forecast the exact irradiance and load profiles at any time.

The following plots show an example of ideal system behaviour according to the data and equations described in the previous chapters (the reference taken here is Zinc-Bromine battery - Rotterdam - Single house with gas heating - 90% self-consumption).

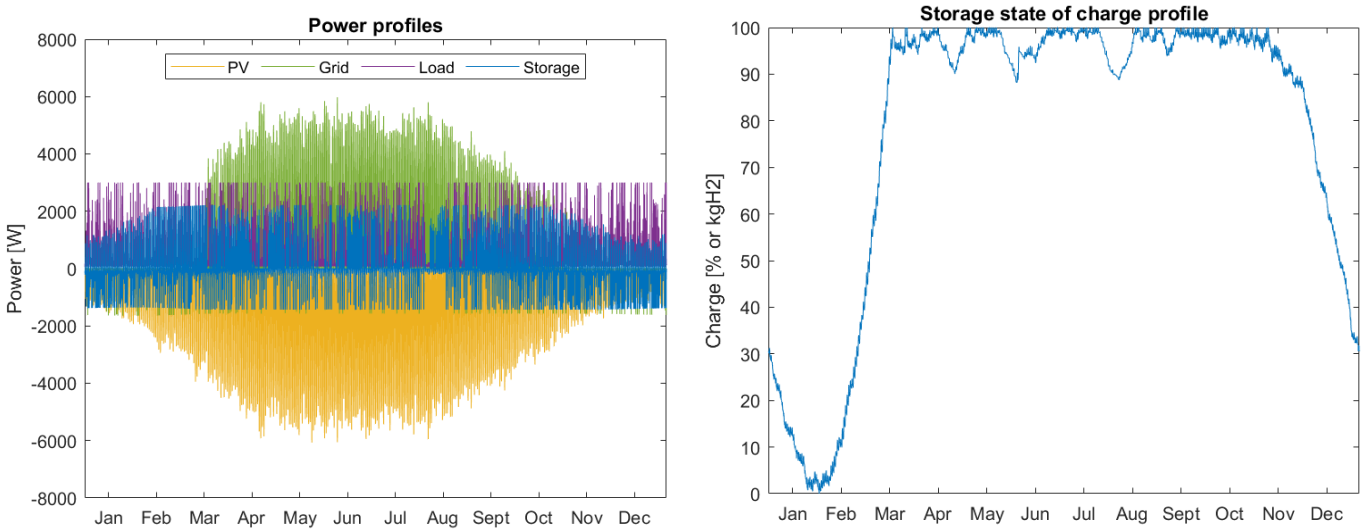

Figure 5.2: Example of optimization model result in yearly plots: power profiles (left) and SOC profile (right)

A full overview of the power flows throughout the year is given in Figure 5.2. In the left graph, the negative side corresponds to power flowing into the system (produced by PV, discharged by the battery or bought from the grid), while the positive side shows power taken out from the system (used by the load, stored in the battery or sold to the grid). Ideally, the storage device (blue) is able to cover a substantial part of the load (purple) and to take up as much solar excess power (yellow) as possible. The load or solar power fraction that the battery is not able to cover, is handled by the grid (green).

The seasonal storage action is evident in the annual state of charge profile on the right: the SOC is kept close to 100% for most of the year (where it has the maximum discharge power) while all the energy capacity is exploited in the least sunny period.

A closer look at the daily profiles is showed in Figure 5.3, where the 21st day of each month are plotted consecutively. The sign convention is the same as before, and here we can observe the daily storage action: the storage device mainly charges during the sunny hours, and discharges in the evening or morning in correspondence to load peaks.

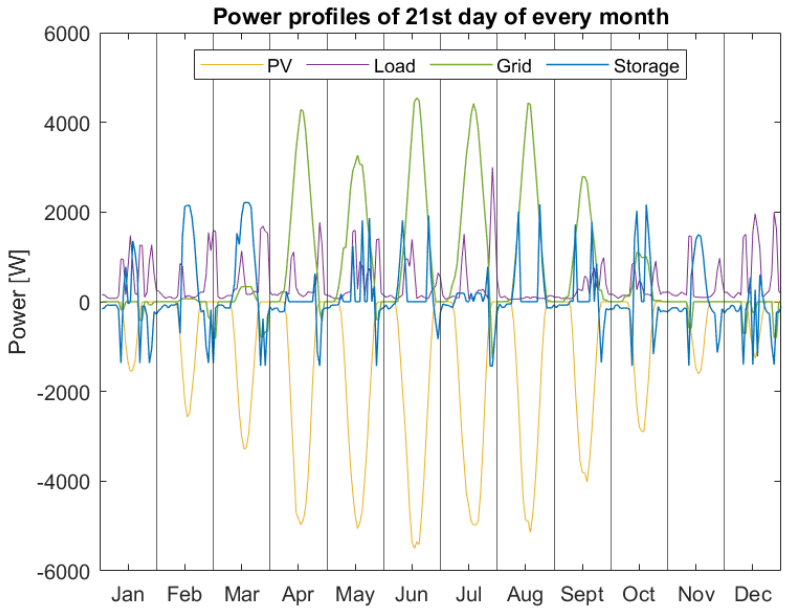

Figure 5.3: Example of optimization model result in yearly plots: power profiles of the 21st day of each month

5.3. Present scenario results

The optimization results in the present scenario finally allow to determine the cost of implementing a residential PV-storage system using the four different technologies, and to identify the differences between them.

5.3.1. LCOE present results

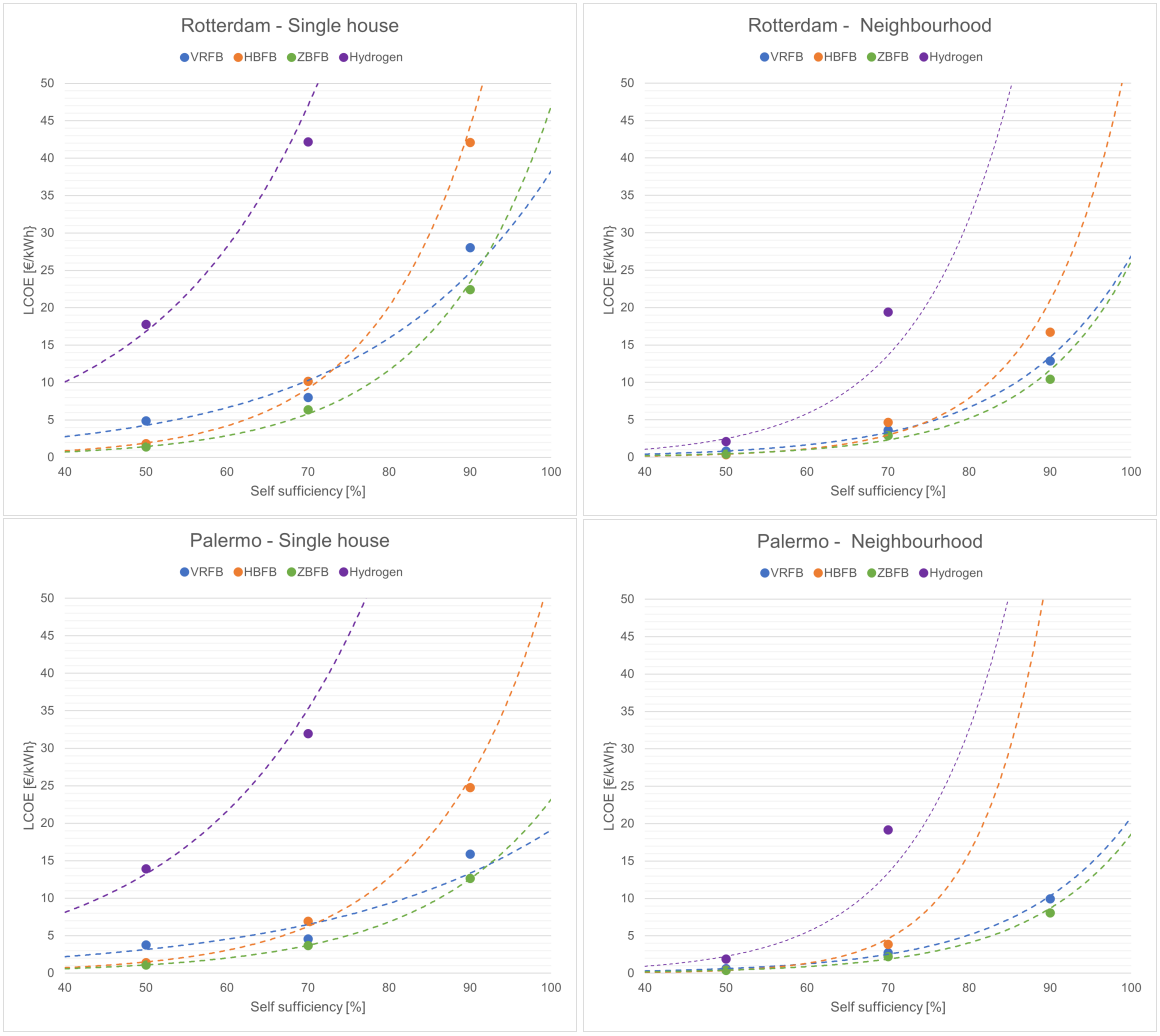

Figure 5.4: LCOE results and trends as function of self-consumption for each battery type in the present day scenarios

In Figure 5.4, the dots represent the calculated LCOE of the system employing each technology (indicated by the color) at three levels of self-consumption. The dashed lines indicate the cost exponential trend in the whole 50-100% self-consumption interval. Costs higher than 50 €/kWh are not shown in favor of a clearer view of lower costs.

From an economic point of view, the obtained costs are all above the current electricity prices (0.1361 €/kWh in the Netherlands and 0.2153 €/kWh in Italy), therefore no solution can be considered economically feasible in the present day scenario. However, it is worth analysing the differences between the battery types. It is evident that the hydrogen system is significantly more expensive than the others, followed by the HBFB, while the ZBFB and VRFB are equally less expensive. This can be explained in different ways:

- The specific cost of hydrogen-based technologies is higher, because they are affected by its low volumetric density and they require tanks, a cooling system and specific piping.
- The hydrogen system currently has a very low round-trip efficiency (around 50%) compared to the other devices. The HBFB has a slightly lower efficiency too.
- The hydrogen-bromine and water splitting-reforming standard voltages are the lowest ones (1.1 and 1.23 V respectively), and these reactions suffer from relatively high resistance losses.

Therefore we can conclude that the VRFB and ZRFB are currently more performing than hydrogen-based systems for residential seasonal applications. In particular, the ZRFB stands out as the most convenient to use.

5.3.2. Battery utilisation

The energy storage technologies studied in this thesis are still in their developing phase and, as described in Chapter 4, their prices are still quite high for an investment in the residential environment. The optimization results of the present scenario clearly show that the revenues coming from storing excess PV power for later use do not compensate the expense of installing such a storage device. In other words, unless the system is forced to make use of storage to reach a high level of self-consumption, it is not convenient to make use of storage, but rather to invest in (cheaper) photovoltaic panels to reduce the electric bill cost.

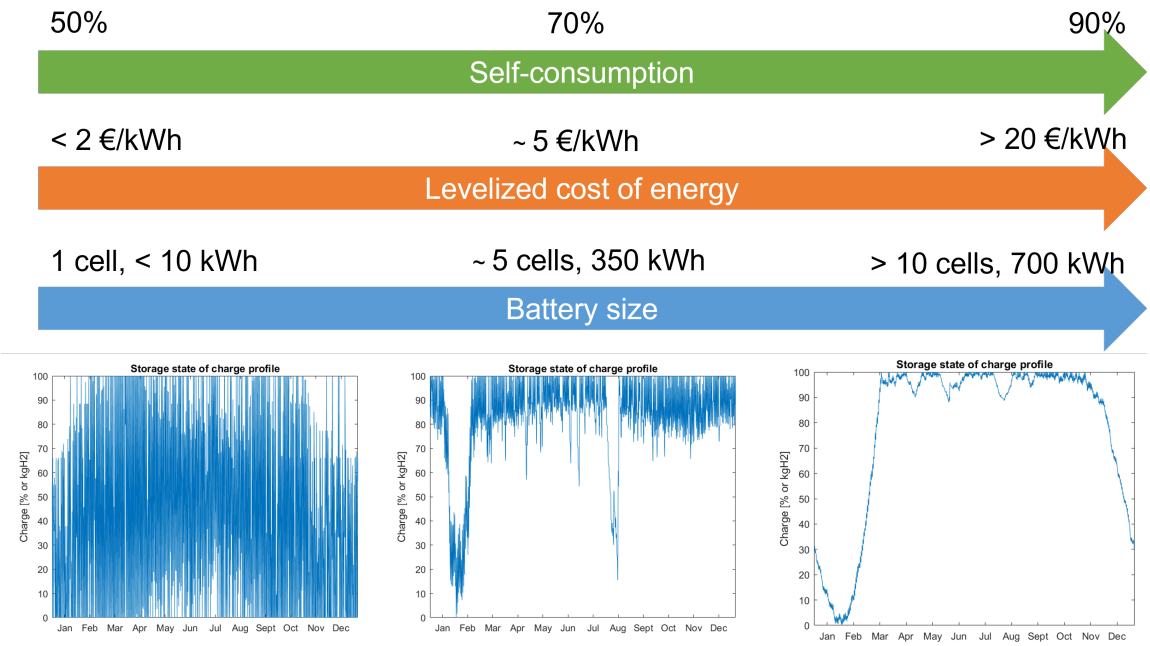

Figure 5.5: Correspondence between self-consumption level, cost, battery size and battery capacity utilization

The results show a clear correspondence between self-consumptionf level, cost and battery sizing, as described in Figure 5.5 (numerical values and graphs correspond to the ZBFB). Here we can clearly see that increasing the self-consumption (SC), the need for storage determines an increase in battery size, that in turns makes the cost rise. From the SOC plots we can infere that the seasonal storage action is exploited only in these cases, while the battery essentially has no purpose at low SC.

5.4. Future results

As explained in the introduction of this chapter, future simulation include a wide series of scenarios and incentive patterns. This time, results are presented using Box & Whisker diagrams as cost ranges divided by case. Each bar represents the cost range from lower to higher self-consumption levels of the technology in the indicated case. The relative "height" of the bar is taken from sample VRFB results and adapted to all the other types.

5.4.1. Present/Future comparison

Firstly, let us compare the present and future results collected in Figure 5.6, where the red horizontal line represents the market electricity price for comparison.

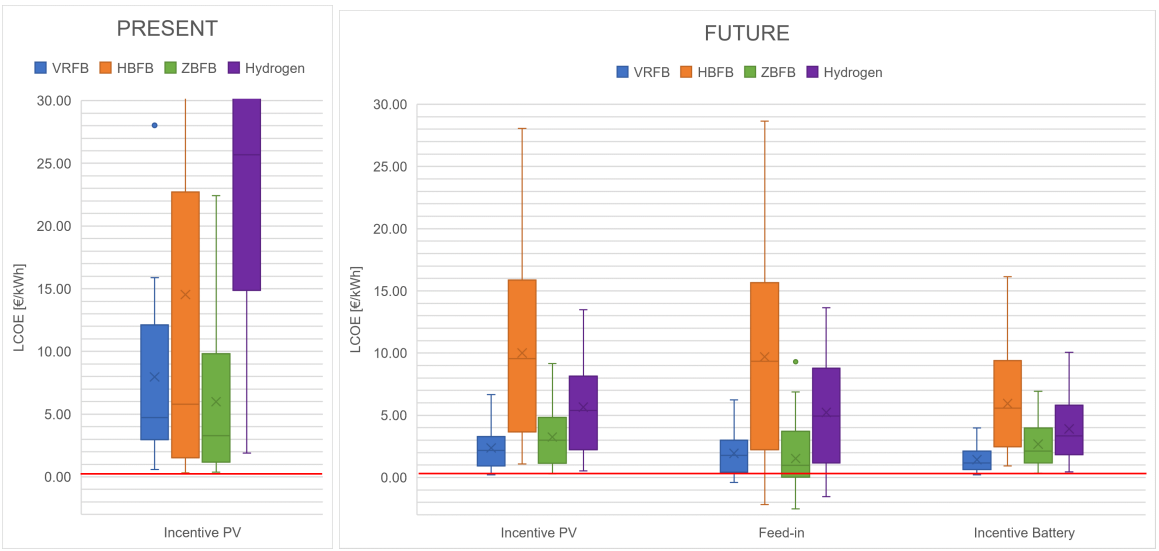

Figure 5.6: Comparison of present and future LCOE results for different types of incentives

The battery investment costs drop and efficiency improvements lead to a clear decrease of levelized costs. In particular, the hydrogen system experiences a great cost reduction, probably due to the optimistic future developments in terms of performance improvement and cost reduction.

5.4.2. LCOE future results

In the following page, a complete overview of the results in each case is provided. Major differences are observed between the neighbourhood and single house case, the latter being less convenient. Regarding the location, Palermo is unsurprisingly more convenient than Rotterdam, due to the greater solar irradiance, hence PV power produced. It is also worth mentioning that the difference between gas and electric heating is minimal - this means that the system is not very sensitive to energy consumption changes, but rather to power distribution (a single home has a more irregular load profile than the neighbourhood).

A few other observations regarding the different storage technologies can be made looking at Figure 5.7:

- The hydrogen-bromide is still the less effective and convenient technology, probably due to its poor expected efficiency improvement.
- The VRFB and ZBFB, on the other hand, prove to be the best solutions even for the future, with an average LCOE of less than 3 €/kWh. In some cases their levelized cost is very close to the market price of electricity. In the feed-in incentive scenario even some negative prices are obtained, meaning that the prosumer actually earns money from the system.
- Knowing that hydrogen systems are probably the most studied technologies between the four, the great cost improvement of hydrogen is an exceptionally promising result.

Nevertheless, it must be pointed out that even these future results cannot be interpreted as feasible, as in most of the cases the prices for a high self-consumption are far from the market prices of electricity. However, the situation could change in case governments adopt stronger or allow to combine them. For example, a combination of feed-in tariff and incentive on the battery installation would probably have a greater benefit on the price than the sum of their single ones.

Figure 5.7: LCOE results collection in different future incentive scenarios for each battery type

6 Conclusions

The increasing levels of CO_2 in the atmosphere released by fossil fuels and the rising global energy demand are leading us to the use of renewable sources, like wind and photovoltaic. The unreliability and instability of these energy sources, however, is an important issue that can be solved by incorporating energy storage, particularly in the residential environment.

Introducing a storage device in a residential system equipped with PV has several technical and economic advantages, especially for the house owner. In particular, storage technologies that are able to retain large amounts of energy for long times can be employed for seasonal storage. Among all the available storage technologies, the most suitable for this purpose are found to be the redox flow batteries (in particular the all-vanadium RFB, the hydrogen-bromide RFB and the zinc-bromide RFB) and the hydrogen system composed by electrolyser, hydrogen tank and fuel cell.

The system described in this work is composed by four main units:

- Load: a single house or small neighbourhood that consumes electricity. This has been modeled thanks to the *LoadProfileGenerator* software.
- Generator: photovoltaic panels, the type considered in this work is crystallyne-Silicon with standard efficiency of 19.2%. They have been modeled starting from average annual weather data including irradiance, air temperature and wind speed.
- Storage: the 4 types of storage devices considered. They have all been modeled starting from their basic structure, the electrochemical cell. Losses are taken from literature and validated against technical specification of commercially available devices.
- Grid: a connection point to the main grid. A passive component modelled from the power balance equation.

In order to determine the economical feasibility of these storage technologies, an optimization model was built, reproducing the control logic of a microgrid system based on power balance and self-consumption. The economic indicator used is the levelized cost of energy, a measure of the lifetime cost of an investment project.

The present and future cost of each component was then determined from literature. The missing prices for the storage devices were assumed by similarities or deduction.

The optimization results showed that in the present scenario none of the technologies has a feasible price to be profitably installed in a residential system. Among the different types, the vanadium and zinc-bromide batteries have the lowest prices, while hydrogen is extremely expensive in the present. On the other hand, in the future scenario several types of incentives were simulated. Technical improvements and cost reductions of the batteries lead to an important drop in levelized cost, that in some cases becomes close to the market price of electricity, especially in the neighbourhood case and in Palermo. The zinc-bromide and vanadium batteries remain the most convenient ones, while the hydrogen system shows a dramatic improvement from the present to the future scenario.

In conclusion, a PV-storage solution using these technologies is very inconvenient in the present, and only in some cases it can be considered convenient in the future. Further improvement in manufacturing costs and performance of the storage devices could certainly lead to an increased feasibility. Moreover, a combination of *ad-hoc* incentives to promote storage utilization in houses could be the determining factor for redox-flow batteries or hydrogen storage implementation in the residential sector.

Some recommendations for future studies are:

- Try combining more incentive types to observe their influence on cost
- Incorporate Time Of Use tariffs in the model to understand the potential of time shifting and energy trading
- Increase the number of houses in a neighbourhood to observe the economic potential of sharing a storage system

Despite the results of this work may not seem very optimistic, thanks to technical improvements and investments in sustainable energy solutions, I am sure we will have the possibility to incorporate these technologies in our energy system, taking advantage of their many benefits.

Appendices

A. GAMS Code

The following code has been used for the optimization in GAMS. Items between square brackets ([ ]) are replaced with data according to the simulation scenario.

```
****** Initial parameters *******
Set t hours /t1*t8760/;
Scalar minSS Desired self-sufficiency of the system /[#]/;
Scalar bigM Utility number for conditional statement /1e5/;

******* Location - related parameters *******
Scalar IP /[#]/, OP /[#]/;
Scalar IGi /[#]/, OGi /[#]/;
Scalar IGo /[#]/, OGo /[#]/;
Scalar F Compound interest rate factor for r = 0.04 and
lifetime = 20;
   F = [#];

****** Data imported from Excel *******
Parameter data(t,*) Load consumption
   $call GDXXRW [FILENAME].xlsx trace=3 par=data rng=A1:D8760
rdim=1 cdim=1
   $gdxin [FILENAME].gdx
   $load data
   $gdxin

Scalar kWhL Load energy consumption;
   kWhL = sum(t, data(t,'Load'))/1000;

******* Storage parameters *******
Scalar cellA Cell active area in m2^ /[#]/;
Scalar Pcmin Cell min charge power /[#]/;
Scalar PcMAX Cell max charge power /[#]/;
Scalar Pdmin Cell min discharge power /[#]/;
Scalar PdMAX Cell max discharge power /[#]/;
Scalar effc Charge efficiency /[#]/;
Scalar effd Discharge efficiency /[#]/;
Scalar c0 Coefficient for charge power calculation wrt SOC
/[#]/;
```

```
Scalar c1 Coefficient for charge power calculation wrt SOC
/[#]/;
Scalar d0 Coefficient for discharge power calculation wrt SOC
/[#]/;
Scalar d1 Coefficient for discharge power calculation wrt SOC
/[#]/;
Scalar IS /[#]/, ISn /[#]/, ISp /[#]/, ISe /[#]/, OS /[#]/;

Variables LCOE Levelized cost of energy
Variables CostP, CostS, CostG Costs of single components
Variables SOC(t) State of charge of storage system
Variables SS Self sufficiency

Positive Variables A Area of PV panels
Positive Variables N Number of cells of storage system
Positive Variables pSdMAX(t), pScMAX(t) Max discharge and
charge power
Positive Variables ES(t) Energy content of storage at time t
Positive Variables kWhS Energy capacity of storage
Positive Variables kWhGi, kWhGo Energy bought of sold back to
the grid
Positive Variables pP(t) Photovoltaic power
Positive Variables pPL(t) Photovoltaic power going to the load
Positive Variables pSd(t) Storage power delivered to the load
Positive Variables pSc(t) Storage power stored from PV
Positive Variables pGi(t) Power bought from the grid
Positive Variables pGo(t) Power sold back to the grid;

Binary Variable U(t) Storage charge-discharge mode switch;

pSdMAX.lo(t) = Pdmin; pSdMAX.up(t) = PdMAX;
pScMAX.lo(t) = Pcmin; pScMAX.up(t) = PcMAX;
SOC.lo(t) = 0; SOC.up(t) = 100;
U.l(t) = data(t,'U');

********* Single house/Neighbourhood **********
*** Single House ***
A.lo = 1; A.up = 50;
N.lo = 1; N.up = 100;
kWhGi.up = 50000; kWhGo.up = 50000;
kWhS.lo = 1; kWhS.up = 5000;

*** Nieghbourhood ***
A.lo = 1; A.up = 500;
N.lo = 1; N.up = 100;
kWhGi.up = 500000; kWhGo.up = 500000;
```

```
kWhS.lo = 100; kWhS.up = 50000;

Equations
   P Definition of PV power
   U1 Definition of storage charge-discharge switching vari-
able
   U2 Definition of storage charge-discharge switching vari-
able
   MAXd Calculation of max discharge power wrt SOC
   MAXc Calculation of max charge power wrt SOC
   Sd Definition of storage discharge power
   Sc Definition of storage charge power
   DES Change in energy content of storage
   Ch Definition of state of charge of storage
   EGi Calculation of energy bought from the grid
   EGo Calculation of energy solf back to the grid
   BalP Balance of PV power
   BalL Balance of load power
   Bal Total system balance
   SSuff Definition of self sufficience
   SSuffLim Self sufficience limit imposition
   CP Calcualtion of PV cost
   CS Calculation of storage cost
   CG Calculation of grid cost
   OBJ Total LCOE cost;

P(t).. pP(t) =e= data(t,'PVm2') * A;

U1(t).. data(t,'Load') - pP(t) =l= bigM * U(t);
U2(t).. pP(t) - data(t,'Load') =l= bigM * (1-U(t));

MAXd(t).. pSdMAX(t) =e= d0 + d1*SOC(t);
MAXc(t).. pScMAX(t) =e= c0 + c1*SOC(t);
Sd(t).. pSd(t) =l= N * pSdMAX(t) * U(t);
Sc(t).. pSc(t) =l= N * pScMAX(t) * (1 - U(t));
DES(t).. ES(t++1) =e= ES(t) - pSd(t)/effd + pSc(t)*effc;
Ch(t).. SOC(t) =e= (ES(t) / (1000*kWhS)) * 100;

EGi.. kWhGi =e= sum(t, pGi(t)/1000);
EGo.. kWhGo =e= sum(t, pGo(t)/1000);

BalP(t).. pP(t) =e= pPL(t) + pSc(t) + pGo(t);
BalL(t).. data(t,'Load') =e= pPL(t) + pSd(t) + pGi(t);
Bal(t).. pP(t) - data(t,'Load') + pSd(t) - pSc(t) + pGi(t) -
pGo(t) =e= 0;
```

```
SSuff.. SS =e= 1 - (kWhGi / kWhL);
SSuffLim.. SS =g= minSS;

CP.. CostP =e= (IP + OP*F)*A;
CS.. CostS =e= (IS + ISn*cellA*N + ISp*N*PcMAX + ISe*kWhS) *
(1 + OS*F);
CG.. CostG =e= IGi + OGi*F*kWhGi + IGo + OGo*F*kWhGo;
OBJ.. LCOE =e= (CostP + CostS + CostG) / (kWhL*F);

Model PVStorage /all/;

Option epsmip = 1.0e-3;

Solve PVStorage using MINLP minimizing LCOE
```

B. Complete Results

A complete collection of all the simulation results is given in the following tables. The notation used here is the following:

- SH = Single house, NB = Neighbourhood
- GH = Gas heating, EH = Electric heating

Numbers written in red represent the lower or upper limit for that variable. In the future scenario, the PV panels area, number of cells and energy capacity have been calculated only at 75% self-consumption.

		LCOE [€/kWh]				PV panels area [m^2]				Number of cells				Energy capacity [kWh]								
	SC [%]	VRFB	HBFB	ZBFB	Hydrogen	VRFB	HBFB	ZBFB	Hydrogen	VRFB	HBFB	ZBFB	Hydrogen	VRFB	HBFB	ZBFB	Hydrogen					
ROTTERDAM	SHGH	50	4.86	1.83	1.38	17.78	44.03	49.44	42.62	41.25	1.00	1.00	1.00	1.00	1.00	1.00	1.00	1.00	1.00	1.00	1.00	1.82
		70	7.98	10.17	6.34	42.17	50.00	50.00	50.00	50.00	1.64	6.07	5.29	2.79	17.27	62.78	14.59	415.88				
		90	28.04	42.10	22.42	138.76	50.00	49.91	50.00	50.00	5.38	25.44	16.86	10.07	240.63	296.43	250.33	788.04				
	NBGH	50	0.79	0.33	0.41	2.08	176.65	236.88	498.69	499.14	1.33	1.00	1.00	1.00	15.32	1.00	1.00	1.36				
		70	3.59	4.67	2.89	19.41	500.00	500.00	500.00	500.00	6.92	27.65	22.85	11.75	67.53	88.69	23.14	2393.55				
		90	12.86	16.72	10.42	62.50	500.00	493.01	500.00	500.00	20.68	92.10	65.29	40.97	2221.81	2053.60	1964.74	5915.77				
PALERMO	SHGH	50	3.76	1.41	1.10	13.90	24.72	33.94	36.16	42.67	1.00	1.00	1.00	1.00	1.41	1.00	1.00	1.71				
		70	4.57	6.91	3.68	31.96	50.00	50.00	50.00	50.00	1.19	5.48	3.90	2.69	14.04	17.07	6.93	211.79				
		90	15.88	24.73	12.63	98.56	50.00	50.00	50.00	50.00	4.30	20.21	14.11	8.91	30.88	43.42	15.95	461.35				
	NBGH	50	0.60	0.42	0.38	1.90	187.87	490.05	497.24	497.24	1.00	1.00	1.00	1.00	1.63	1.00	1.00	1.61				
		70	2.75	3.85	2.21	19.17	500.00	500.00	500.00	500.00	5.73	24.84	18.81	12.95	61.72	90.41	23.12	1254.92				
		90	9.94	61.29	8.06	66.30	500.00	500.00	500.00	500.00	22.29	100.00	75.22	48.78	215.37	50000.00	88.83	2940.32				

Figure B.1: Complete collection of optimization results in the present day scenario

Location	Building	Inventive type	SC [%]	LCOE [€/kWh] VRFB	LCOE [€/kWh] HBFB	LCOE [€/kWh] ZBFB	LCOE [€/kWh] Hydrogen	PV panels area [m^2] VRFB	PV panels area [m^2] HBFB	PV panels area [m^2] ZBFB	PV panels area [m^2] Hydrogen	Number of cells VRFB	Number of cells HBFB	Number of cells ZBFB	Number of cells Hydrogen	Energy capacity [kWh] VRFB	Energy capacity [kWh] HBFB	Energy capacity [kWh] ZBFB	Energy capacity [kWh] Hydrogen
ROTTERDAM	NBGH	Incentive PV	50	0.29	1.15	0.54	0.67	500.00	500.00	215.83	500.00	5.84	35.93	4.52	14.26	18.58	910.34	10.20	2268.85
			75	1.69	6.71	3.14	3.94												
			90	3.08	12.28	5.73	7.20												
		Feed-in	50	-0.13	-0.63	-0.01	-0.34	500.00	500.00	500.00	500.00	5.82	35.74	3.76	14.26	18.91	931.76	6.92	2268.85
			75	1.29	6.45	0.14	3.50												
			90	2.70	13.54	0.28	7.35												
		Incentive Battery	50	0.42	1.50	1.14	0.83	500.00	500.00	221.54	500.00	5.82	41.70	4.48	14.26	19.06	249.50	10.26	2268.85
			75	1.15	4.12	3.13	2.28												
			90	1.89	6.75	5.12	3.73												
	NBEH	Incentive PV	50	0.22	1.09	0.29	0.53	500.00	500.00	465.39	500.00	13.87	70.62	9.85	26.95	45.67	5390.15	11.87	5626.50
			75	1.79	9.04	2.42	4.38												
			90	3.37	16.99	4.55	8.24												
		Feed-in	50	0.00	0.01	0.00	0.01	500.00	500.00	500.00	500.00	14.02	70.17	9.72	26.95	43.73	5364.59	11.76	5626.50
			75	1.53	8.89	1.33	4.19												
			90	3.07	17.77	2.66	8.38												
		Incentive Battery	50	0.22	0.97	0.44	0.46	500.00	500.00	465.39	500.00	14.40	70.67	9.84	27.17	44.71	5392.92	11.87	5578.99
			75	1.21	5.34	2.42	2.52												
			90	2.19	9.70	4.40	4.58												

Location	Building	Inventive type	SC [%]	LCOE [€/kWh] VRFB	LCOE [€/kWh] HBFB	LCOE [€/kWh] ZBFB	LCOE [€/kWh] Hydrogen	PV panels area [m^2] VRFB	PV panels area [m^2] HBFB	PV panels area [m^2] ZBFB	PV panels area [m^2] Hydrogen	Number of cells VRFB	Number of cells HBFB	Number of cells ZBFB	Number of cells Hydrogen	Energy capacity [kWh] VRFB	Energy capacity [kWh] HBFB	Energy capacity [kWh] ZBFB	Energy capacity [kWh] Hydrogen
ROTTERDAM	SHGH	Incentive PV	50	1.40	5.55	1.48	2.71	50.00	50.00	50.00	50.00	1.23	9.75	6.61	3.49	16.49	87.76	93.45	352.09
			75	4.03	15.95	4.25	7.78												
			90	6.65	26.35	7.01	12.85												
		Feed-in	50	1.02	4.36	1.12	2.06	50.00	50.00	50.00	50.00	1.23	9.65	6.60	3.49	16.15	86.61	93.44	352.09
			75	3.63	15.55	4.00	7.36												
			90	6.24	26.75	6.88	12.66												
		Incentive Battery	50	0.93	3.60	1.62	1.68	50.00	50.00	50.00	50.00	1.25	9.83	6.67	3.49	16.34	91.01	93.58	325.09
			75	2.46	9.49	4.28	4.43												
			90	3.98	15.38	6.94	7.18												
	SHEH	Incentive PV	50	0.62	3.36	1.10	1.61	50.00	50.00	50.00	50.00	3.36	15.63	14.15	6.05	789.21	1984.53	1583.81	1853.29
			75	2.89	15.71	5.12	7.55												
			90	5.16	28.06	9.15	13.48												
		Feed-in	50	0.48	2.73	0.89	1.30	50.00	50.00	50.00	50.00	3.39	15.63	14.15	6.50	749.32	1984.53	1583.82	1853.29
			75	2.78	15.69	5.10	7.47												
			90	5.08	28.64	9.30	13.63												
		Incentive Battery	50	0.43	2.31	1.29	1.07	50.00	50.00	50.00	50.00	3.63	15.63	14.15	6.50	671.66	1984.56	1583.83	1835.29
			75	1.73	9.22	5.13	4.27												
			90	3.03	16.13	8.96	7.46												

Figure B.2: Complete collection of optimization results in the future scenario - Rotterdam

PALERMO																	
			NBGH				NBEH				NBGH				NBEH		
Inventive type	SC [%]	LCOE [€/kWh]				PV panels area [m^2]				Number of cells				Energy capacity [kWh]			
		VRFB	HBFB	ZBFB	Hydrogen	VRFB	HBFB	ZBFB	Hydrogen	VRFB	HBFB	ZBFB	Hydrogen	VRFB	HBFB	ZBFB	Hydrogen
Incentive PV	50	0.35	1.22	0.60	0.95	379.32	500.00	126.66	379.32	5.65	37.69	5.53	17.38	40.55	158.50	6.04	1288.74
	75	1.63	5.65	2.76	4.39												
	90	2.90	10.08	4.93	7.84												
Feed-in	50	-0.39	-2.17	1.05	-1.55	379.32	500.00	500.00	379.32	5.68	38.58	5.15	17.38	34.54	139.62	7.16	1288.74
	75	0.93	5.20	-2.52	3.71												
	90	2.26	12.56	-6.09	8.97												
Incentive Battery	50	0.30	1.01	0.48	0.74	378.99	500.00	62.69	379.32	5.93	39.18	5.85	17.38	23.51	110.02	10.01	1288.74
	75	1.01	3.41	1.64	2.50												
	90	1.73	5.81	2.79	4.26												
Incentive PV	50	0.30	1.11	0.41	0.81	370.43	500.00	211.45	370.43	9.23	60.02	6.82	24.60	42.85	164.13	27.01	3007.79
	75	1.66	6.23	2.32	4.56												
	90	3.02	11.36	4.23	8.31												
Feed-in	50	-0.19	-0.88	0.18	-0.64	370.43	500.00	500.00	370.43	9.32	57.91	6.41	24.60	38.09	216.74	26.12	3007.79
	75	1.23	5.70	-1.16	4.14												
	90	2.65	12.29	-2.50	8.91												
Incentive Battery	50	0.25	0.92	0.35	0.63	370.43	500.00	159.28	370.43	12.68	62.49	7.11	24.60	55.64	87.50	27.71	3007.79
	75	1.01	3.75	1.41	2.58												
	90	1.78	6.58	2.48	4.53												

PALERMO																	
		SHEH				SHGH				SHEH				SHGH			
Inventive type	SC [%]	LCOE [€/kWh]				PV panels area [m^2]				Number of cells				Energy capacity [kWh]			
		VRFB	HBFB	ZBFB	Hydrogen	VRFB	HBFB	ZBFB	Hydrogen	VRFB	HBFB	ZBFB	Hydrogen	VRFB	HBFB	ZBFB	Hydrogen
Incentive PV	50	1.19	4.57	1.23	2.74	50.00	50.00	50.00	50.00	1.05	8.66	6.07	3.54	12.71	25.32	11.37	187.87
	75	2.79	10.75	2.89	6.46												
	90	4.39	16.92	4.55	10.17												
Feed-in	50	0.40	2.06	0.49	1.14	50.00	50.00	50.00	50.00	1.05	8.66	6.08	3.54	12.81	25.33	11.36	187.87
	75	2.00	10.30	2.45	5.69												
	90	3.60	18.54	4.40	10.23												
Incentive Battery	50	0.76	2.91	0.77	2.96	50.00	50.00	50.00	50.00	1.05	8.80	6.09	3.54	13.93	24.89	11.36	187.87
	75	0.79	6.35	1.68	6.46												
	90	2.57	9.78	2.59	9.95												
Incentive PV	50	0.85	3.36	1.04	2.08	49.91	50.00	50.00	50.00	1.93	11.53	10.12	4.44	26.67	187.01	36.79	721.42
	75	2.54	10.06	3.12	6.23												
	90	4.22	16.76	5.20	10.37												
Feed-in	50	0.35	1.64	0.48	0.97	50.00	50.00	50.00	50.00	1.94	11.88	10.10	4.44	26.89	134.22	36.71	721.42
	75	2.07	9.82	2.87	5.78												
	90	3.79	18.00	5.26	10.60												
Incentive Battery	50	0.58	2.23	0.69	2.38	50.00	50.00	50.00	50.00	1.97	11.90	10.22	4.44	23.64	134.19	37.33	721.42
	75	1.52	5.85	1.80	6.23												
	90	2.46	9.46	2.91	10.07												

Figure B.3: Complete collection of optimization results in the future scenario - Palermo

List of Figures

List of Tables

References

[1] IEA. *Global Energy Review 2019*. Paris, 2020. URL: https://www.iea.org/reports/global-energy-review-2019.

[2] IEA. *Global Energy & CO2 Status Report 2019*. Paris, 2019. URL: https://www.iea.org/reports/global-energy-co2-status-report-2019.

[3] E. Commission. *A European Green Deal*. 2019. URL: https://ec.europa.eu/info/strategy/priorities-2019-2024/european-green-deal.

[4] IEA. *World Energy Outlook 2017*. Paris, 2017. URL: https://www.iea.org/reports/world-energy-outlook-2017.

[5] *Solar vs. Wind Power Comparison | Which One Is Better for Your Home?* 2020. URL: https://www.axionpower.com/knowledge/solar-vs-wind/.

[6] IEA. *Renewables 2019*. Paris, 2019. URL: https://www.iea.org/reports/renewables-2019.

[7] IEA. *World Energy Balances 2020: Data and Statistics*. Paris, 2020. URL: https://www.iea.org/data-and-statistics?country=WEOEUR&fuel=Energy%5C%20consumption&indicator=TFCShareBySector.

[8] M. C. Argyrou, P. Christodoulides, and S. A. Kalogirou. ``Energy storage for electricity generation and related processes: Technologies appraisal and grid scale applications". In: *Renewable and Sustainable Energy Reviews* 94 (2018), pp. 804–821. ISSN: 1364-0321. DOI: https://doi.org/10.1016/j.rser.2018.06.044.

[9] V. Vega-Garita et al. ``Review of residential PV-storage architectures". In: *2016 IEEE International Energy Conference (ENERGYCON)*. 2016, pp. 1–6. DOI: http://dx.doi.org/10.1109/ENERGYCON.2016.7514039.

[10] H. Hesse et al. ``Lithium-Ion Battery Storage for the Grid—A Review of Stationary Battery Storage System Design Tailored for Applications in Modern Power Grids". In: *Energies* 10 (Dec. 2017), p. 2107. DOI: https://doi.org/10.3390/en10122107.

[11] Eurelectric. *Decentralised storage: impact on future distribution grids*. 2012. URL: https://www.eurelectric.org/media/1730/eurelectric_decentralized_storage_finalcover_dcopy-2012-030-0574-01-e.pdf.

[12] X. Luo et al. ``Overview of current development in electrical energy storage technologies and the application potential in power system operation". In: *Applied Energy* 137 (2015), pp. 511–536. ISSN: 0306-2619. DOI: https://doi.org/10.1016/j.apenergy.2014.09.081.

[13] S. Sabihuddin, A. E. Kiprakis, and M. Mueller. ``A Numerical and Graphical Review of Energy Storage Technologies". In: *Energies* 8.1 (2015), pp. 172–216. ISSN: 1996-1073. DOI: https://doi.org/10.3390/en8010172.

[14] I. E. Commission. *IEC White Paper: Electrical Energy Storage*. Geneva, 2011. URL: https://basecamp.iec.ch/download/iec-white-paper-electrical-energy-storage/.

[15] T. Grejtak. *Defining and Scouting Long-duration Energy Storage: Because "More Than Four Hours" Isn't Enough*. 2018.

[16] T. M. Gür. ``Review of electrical energy storage technologies, materials and systems: challenges and prospects for large-scale grid storage". In: *Energy & Environmental Science* 11 (10 2018), pp. 2696–2767. DOI: https://doi.org/10.1039/C8EE01419A.

[17] P. Medina et al. ``Electrical Energy Storage Systems: Technologies' State-of-the-Art, Techno-economic Benefits and Applications Analysis". In: *2014 47th Hawaii International Conference on System Sciences*. 2014, pp. 2295–2304. DOI: https://doi.org/10.1109/HICSS.2014.290.

[18] M. Yekini Suberu, M. Wazir Mustafa, and N. Bashir. ``Energy storage systems for renewable energy power sector integration and mitigation of intermittency". In: *Renewable and Sustainable Energy Reviews* 35 (2014), pp. 499–514. ISSN: 1364-0321. DOI: https://doi.org/10.1016/j.rser.2014.04.009.

[19] A. Joseph and M. Shahidehpour. ``Battery storage systems in electric power systems". In: *2006 IEEE Power Engineering Society General Meeting*. 2006, 8 pp.-. DOI: https://doi.org/10.1109/PES.2006.1709235.

[20] H. Chen et al. ``Progress in electrical energy storage system: A critical review". In: *Progress in Natural Science* 19.3 (2009), pp. 291–312. ISSN: 1002-0071. DOI: https://doi.org/10.1016/j.pnsc.2008.07.014.

[21] D.-B. Steber. ``Integration of Decentralized Battery Energy Storage Systems into the German Electrical Power System". PhD thesis. Friedrich Alexander Universitet Erlangen Nurnberg (FAU), 2018.

[22] N.-K. C. Nair and N. Garimella. ``Battery energy storage systems: Assessment for small-scale renewable energy integration". In: *Energy and Buildings* 42.11 (2010), pp. 2124–2130. ISSN: 0378-7788. DOI: https://doi.org/10.1016/j.enbuild.2010.07.002.

[23] R. M. Herritty and J. Midolo. ``Nickel Cadmium Batteries for Photovoltaic Application". In: *Proceedings of the Annual Battery Conference on Applications and Advances*. Long Beach, CA, USA, 1998. DOI: https://doi.org/10.1016/B978-0-08-037539-7.50020-X.

[24] A. Gallo et al. ``Energy storage in the energy transition context: A technology review". In: *Renewable and Sustainable Energy Reviews* 65 (2016), pp. 800–822. ISSN: 1364-0321. DOI: https://doi.org/10.1016/j.rser.2016.07.028.

[25] M. Beaudin et al. ``Energy storage for mitigating the variability of renewable electricity sources: An updated review". In: *Energy for Sustainable Development* 14.4 (2010), pp. 302–314. ISSN: 0973-0826. DOI: https://doi.org/10.1016/j.esd.2010.09.007.

[26] B. Dunn, H. Kamath, and J.-M. Tarascon. ``Electrical Energy Storage for the Grid: A Battery of Choices''. In: *Science* 334 (2011), pp. 928–935. ISSN: 6058. DOI: https://doi.org/10.1126/science.1212741.

[27] J. Tarascon and M. Armand. ``Issues and challenges facing rechargeable lithium batteries''. In: *Nature* 414 (2001), pp. 359–367. DOI: https://doi.org/10.1038/35104644.

[28] IRENA. *Electricity storage and renewables: Costs and markets in 2030*. Abu Dhabi, 2017.

[29] C. Doetsch and J. Burfeind. ``Chapter 12 - Vanadium Redox Flow Batteries''. In: *Storing Energy*. Ed. by T. M. Letcher. Oxford: Elsevier, 2016, pp. 227–246. ISBN: 978-0-12-803440-8. DOI: https://doi.org/10.1016/B978-0-12-803440-8.00012-9.

[30] G. L. Soloveichik. ``Flow Batteries: Current Status and Trends''. In: *Chemical Reviews* 115.20 (2015), pp. 11533–11558. DOI: https://doi.org/10.1021/cr500720t.

[31] J. Cao et al. ``Organic Flow Batteries: Recent Progress and Perspectives''. In: *Energy & Fuels* 34.11 (2020), pp. 13384–13411. DOI: https://doi.org/10.1021/acs.energyfuels.0c02855.

[32] Y. Wang et al. ``A review on unitized regenerative fuel cell technologies, part B: Unitized regenerative alkaline fuel cell, solid oxide fuel cell, and microfluidic fuel cell''. In: *Renewable and Sustainable Energy Reviews* 75 (2017), pp. 775–795. ISSN: 1364-0321. DOI: https://doi.org/10.1016/j.rser.2016.11.054.

[33] ``Chapter 5.3.3 - Application of Hydrogen by Use of Chemical Reactions of Hydrogen and Carbon Dioxide''. In: *Science and Engineering of Hydrogen-Based Energy Technologies*. Ed. by P. E. V. de Miranda. Academic Press, 2019, pp. 279–289. ISBN: 978-0-12-814251-6. DOI: https://doi.org/10.1016/B978-0-12-814251-6.00013-7.

[34] H. L. Huynh et al. ``Synthetic natural gas production from CO2 and renewable H2: Towards large-scale production of Ni–Fe alloy catalysts for commercialization''. In: *Journal of Cleaner Production* 264 (2020), p. 121720. ISSN: 0959-6526. DOI: https://doi.org/10.1016/j.jclepro.2020.121720.

[35] P. Breeze. ``Chapter 8 - Direct Methanol Fuel Cell''. In: *Fuel Cells*. Ed. by P. Breeze. Academic Press, 2017, pp. 75–82. ISBN: 978-0-08-101039-6. DOI: https://doi.org/10.1016/B978-0-08-101039-6.00008-X.

[36] U. S. D. of Energy. *DOE OE Global Energy Storage Database*. 2020. URL: https://www.sandia.gov/ess-ssl/global-energy-storage-database/.

[37] I. Hadjipaschalis, A. Poullikkas, and V. Efthimiou. ``Overview of current and future energy storage technologies for electric power applications''. In: *Renewable and Sustainable Energy Reviews* 13.6 (2009), pp. 1513–1522. ISSN: 1364-0321. DOI: https://doi.org/10.1016/j.rser.2008.09.028.

[38] X. Luo et al. ``Overview of Current Development in Compressed Air Energy Storage Technology''. In: *Energy Procedia* 62 (2014). 6th International Conference on Sustainability in Energy and Buildings, SEB-14, pp. 603–611. ISSN: 1876-6102. DOI: https://doi.org/10.1016/j.egypro.2014.12.423.

[39] J. Moshövel et al. ``Analysis of the maximal possible grid relief from PV-peak-power impacts by using storage systems for increased self-consumption''. In: *Applied Energy* 137 (2015), pp. 567–575. ISSN: 0306-2619. DOI: https://doi.org/10.1016/j.apenergy.2014.07.021.

[40] J. Hoppmann et al. ``The economic viability of battery storage for residential solar photovoltaic systems – A review and a simulation model''. In: *Renewable and Sustainable Energy Reviews* 39 (2014), pp. 1101–1118. ISSN: 1364-0321. DOI: https://doi.org/10.1016/j.rser.2014.07.068.

[41] C. Goebel, V. Cheng, and H.-A. Jacobsen. ``Profitability of Residential Battery Energy Storage Combined with Solar Photovoltaics''. In: *Energies* 10.7 (2017). ISSN: 1996-1073. DOI: https://doi.org/10.3390/en10070976.

[42] E. Commission. *Questions and Answers on Sustainable Batteries Regulation*. 2020. URL: https://ec.europa.eu/commission/presscorner/detail/en/qanda_20_2311.

[43] B. Miller. *Materials in lithium-ion batteries may be recycled for reuse*. 2020. URL: https://phys.org/news/2020-09-materials-lithium-ion-batteries-recycled-reuse.html.

[44] E. Commission. *Green Deal: Sustainable batteries for a circular and climate neutral economy*. 2020. URL: https://ec.europa.eu/commission/presscorner/detail/en/ip_20_2312.

[45] N. Pflugradt. *LoadProfileGenerator*. URL: https://www.loadprofilegenerator.de/.

[46] Delft University of Technology. *Dutch PV Portal*. URL: http://dutchpvportal.tudelft.nl/.

[47] Photovoltaic Geographical Information System (PVGIS). URL: https://re.jrc.ec.europa.eu/pvgis.

[48] E. Lorenz et al. ``Regional PV power prediction for improved grid integration''. In: *Progress in Photovoltaics: Research and Applications* 19.7 (2011), pp. 757–771.

[49] Sandia National Lab. *Sandia Module Temperature Model*. URL: https://pvpmc.sandia.gov/modeling-steps/2-dc-module-iv/module-temperature/sandia-module-temperature-model/.

[50] B. Sundén. ``Chapter 2 - Electrochemistry and thermodynamics''. In: *Hydrogen, Batteries and Fuel Cells*. Ed. by B. Sundén. Academic Press, 2019, pp. 15–36. ISBN: 978-0-12-816950-6. DOI: https://doi.org/10.1016/B978-0-12-816950-6.00002-6.

[51] A. J. Bard and L. R. Faulkner. *Electrochemical methods*. Ed. by i. John Wiley & Sons. 2000. ISBN: 978-0-471-04372-0. DOI: https://doi.org/10.1016/B978-0-12-816950-6.00002-6.

[52] B. A. Averill and P. Eldredge. ``Chapter 19 - Electrochemistry''. In: *General Chemistry: Principles, Patterns and Applications*. 2007.

[53] C. Blanc and A. Rufer. ``Multiphysics and energetic modeling of a vanadium redox flow battery''. In: *2008 IEEE International Conference on Sustainable Energy Technologies*. IEEE. 2008, pp. 696–701.

[54] E. Sánchez-Díez et al. ``Redox flow batteries: Status and perspective towards sustainable stationary energy storage''. In: *Journal of Power Sources* 481 (2021), p. 228804. ISSN: 0378-7753. DOI: https://doi.org/10.1016/j.jpowsour.2020.228804.

[55] *H2 Inc. EnerFlow*. URL: http://www.h2aec.com/sub/product/product08.php.

[56] *Volteiron powerRFB*. URL: https://www.volterion.com/en/systems/.

[57] *Golden Energy Century GEC-VFB*. URL: http://www.gec.com.cn/root/web/index.php.

[58] *VFlowTech POWERCUBE*. URL: http://www.vflowtech.com/product-details/10-100-kwh/.

[59] *UniEnergy Technologies ReFlex*. URL: https://uetechnologies.com/.

[60] *VisBlue*. URL: https://visblue.com/product.html.

[61] *Big Pawer*. URL: http://en.bigpawer.com/productdetail.php?id=1233.

[62] *PinFlow*. URL: http://www.pinflowes.com/Products-industry.html.

[63] *StorEn Technologies TitanStack*. URL: https://www.storen.tech/titan-stack-battery.

[64] *Rongke Power Vmodule1-B*. URL: http://www.rongkepower.com/chuneng?lang=en.

[65] *Sumitomo Electric*. URL: https://sumitomoelectric.com/products/redox.

[66] *Cell Cube*. URL: https://www.cellcube.com/the-cellcube-system/.

[67] *Largo Clean Energy*. URL: https://www.largocleanenergy.com/products.

[68] D. Aaron et al. ``Dramatic performance gains in vanadium redox flow batteries through modified cell architecture''. In: *Journal of Power Sources* 206 (2012), pp. 450–453. ISSN: 0378-7753. DOI: https://doi.org/10.1016/j.jpowsour.2011.12.026.

[69] M. Skyllas-Kazacos and C. Menictas. ``The vanadium redox battery for emergency back-up applications''. In: *Proceedings of Power and Energy Systems in Converging Markets*. 1997, pp. 463–471. DOI: 10.1109/INTLEC.1997.645928.

[70] H. Bindner et al. ``Characterization of vanadium flow battery''. In: (2010).

[71] K. T. Cho et al. ``Cyclic performance analysis of hydrogen-bromine flow batteries for grid-scale energy storage". In: *ChemPlusChem* 80.2 (2015), p. 402.

[72] K. T. Cho et al. ``High performance hydrogen/bromine redox flow battery for grid-scale energy storage". In: *Journal of The Electrochemical Society* 159.11 (2012), A1806.

[73] Y. A. Hugo et al. ``Techno-economic analysis of a kilo-watt scale hydrogen-bromine flow battery system for sustainable energy storage". In: *Processes* 8.11 (2020), p. 1492.

[74] *Elestor website*. URL: https://www.elestor.nl/.

[75] E. Manla et al. ``Modeling of zinc bromide energy storage for vehicular applications". In: *IEEE Transactions on Industrial Electronics* 57.2 (2009), pp. 624–632.

[76] I.
bibinitperiod Science. URL: https://www.bsef.com/innovation-science/.

[77] *Redflow ZBM2*. URL: https://redflow.com/resource-category/technical-resources/.

[78] *Primus Power EnergyPod 2*. URL: https://primuspower.com/en/product/.

[79] A. V. da Rosa and J. C. Ordóñez. ``Chapter 10 - Hydrogen Production". In: *Fundamentals of Renewable Energy Processes (Fourth Edition)*. Ed. by A. V. da Rosa and J. C. Ordóñez. Fourth Edition. Oxford: Academic Press, 2022, pp. 419–470. ISBN: 978-0-12-816036-7. DOI: https://doi.org/10.1016/B978-0-12-816036-7.00021-X.

[80] C. H. Arredondo et al. ``Characterization and Application of Agave salmiana Cuticle as Bio-membrane in Low-temperature Electrolyzer and Fuel Cells". In: *Applied Sciences* 9.20 (2019). ISSN: 2076-3417. DOI: https://doi.org/10.3390/app9204461.

[81] K. Zeng and D. Zhang. ``Recent progress in alkaline water electrolysis for hydrogen production and applications". In: *Progress in Energy and Combustion Science* 36.3 (2010), pp. 307–326. ISSN: 0360-1285. DOI: https://doi.org/10.1016/j.pecs.2009.11.002.

[82] A. Buttler and H. Spliethoff. ``Current status of water electrolysis for energy storage, grid balancing and sector coupling via power-to-gas and power-to-liquids: A review". In: *Renewable and Sustainable Energy Reviews* 82 (2018), pp. 2440–2454. ISSN: 1364-0321. DOI: https://doi.org/10.1016/j.rser.2017.09.003.

[83] F. M. Sapountzi et al. ``Electrocatalysts for the generation of hydrogen, oxygen and synthesis gas". In: *Progress in Energy and Combustion Science* 58 (2017), pp. 1–35. ISSN: 0360-1285. DOI: https://doi.org/10.1016/j.pecs.2016.09.001.

[84] O. Schmidt et al. ``Future cost and performance of water electrolysis: An expert elicitation study''. In: *International Journal of Hydrogen Energy* 42.52 (2017), pp. 30470–30492. ISSN: 0360-3199. DOI: https://doi.org/10.1016/j.ijhydene.2017.10.045.

[85] *Angstrom Advanced*. URL: https://www.angstrom-advanced.com/.

[86] *Areva H2Gen*. URL: https://doczz.net/doc/4762105/areva-h2-gen-a-pem-electrolyser-manufacturer---h2bz.

[87] *Giner Inc*. URL: https://www.ginerinc.com/.

[88] *GreenHydrogen*. URL: https://greenhydrogen.dk/.

[89] *Hydrogenics*. URL: https://www.cummins.com/new-power?Sfvrsn=2.

[90] *ITM Power*. URL: https://www.itm-power.com/products.

[91] *Kobelco Eco-Solutions*. URL: https://www.kobelco-eco.co.jp/english/.

[92] *NelHydrogen*. URL: https://nelhydrogen.com/product/c10-c20-c30/.

[93] *McPhy*. URL: https://cellar-c2.services.clever-cloud.com/com-mcphy/uploads/2020/08/20.05.McPhy_Portfolio_ELY_McLyzer_EN.pdf.

[94] *Proton On Site*. URL: https://advanzh2.ca//wp-content/uploads/2018/04/m-series.pdf.

[95] *Pure Energy Centre*. URL: https://pureenergycentre.com/hydrogen-products-pure-energy-centre/hydrogen-electrolyser/.

[96] *Siemens*. URL: https://assets.new.siemens.com/siemens/assets/public.1524040818.abae9c1e48d6d239c06d88e565a25040ed2078dc.ct-ree-18-047-db-silyzer-300-db-de-en-rz.pdf.

[97] *Suzhou Jingli*. URL: https://www.jinglihydrogen.com/water-electrolyzer/water-electrolyzer-dq100.html.

[98] *Taledyne Energy Systems*. URL: http://www.teledynees.com/products/Hydrogen%5C%20Oxygen%5C%20Generation%5C%20Systems/Product%5C%20Files/TESI_Brochure_TITAN_HMXT_Series_English_2013.pdf.

[99] *Treadwell Corporation*. URL: https://www.treadwellcorp.com/.

[100] J. Larminie and A. Dicks. *Fuel Cell Systems Explained - Second edition*. John Wiley & Sons Ltd, 2003.

[101] R. Kortlever. *Electrochemical energy storage course slides*. 2020.

[102] Y. Sanghai. ``Techno-Economic Analysis of Hydrogen Fuel Cell Systems Used as an Electricity Storage Technology in a Wind Farm with Large Amounts of Intermittent Energy''. University of Massachussetts Amherst, 2013. URL: https://core.ac.uk/download/pdf/13638784.pdf.

[103] J. Benziger et al. ``The dynamic response of PEM fuel cells to changes in load''. In: *Chemical Engineering Science* 60.6 (2005), pp. 1743–1759. ISSN: 0009-2509. DOI: https://doi.org/10.1016/j.ces.2004.10.033.

[104] *Ballard*. URL: https://www.ballard.com/fuel-cell-solutions/fuel-cell-power-products/fuel-cell-stacks.

[105] *Elring Kinger*. URL: https://www.elringklinger.com/en/press/publications-and-brochures/e-mobility/fuel-cell-technology.

[106] *Horizon*. URL: https://www.horizonfuelcell.com/fcproducts.

[107] *Nedstack*. URL: https://nedstack.com/en/pem-fcs-stack-technology.

[108] *PlugPower*. URL: https://www.plugpower.com/hydrogen/genfuel/stationary-power/.

[109] R. Griessen and A. Zuttel. ``Chapter IX - Sustainability and hydrogen''. In: *Science and Technology of Hydrogen in Metals*. 2003.

[110] M. Ni. ``An Overview of Hydrogen Storage Technologies''. In: *Energy Exploration Exploitation* 24.3 (2006), pp. 197–209. DOI: https://doi.org/10.1260/014459806779367455.

[111] Fraunhofer ISE. *Current and Future Cost of Photovoltaics. Long-term Scenarios for Market Development, System Prices and LCOE of Utility-Scale PV Systems*. 2015.

[112] C. S. Lai and M. D. McCulloch. ``Levelized cost of electricity for solar photovoltaic and electrical energy storage''. In: *Applied energy* 190 (2017), pp. 191–203. DOI: https://doi.org/10.1016/j.apenergy.2016.12.153.

[113] F. Polzin et al. ``The effect of differentiating costs of capital by country and technology on the European energy transition''. In: *Climatic Change* 167.1 (2021), pp. 1–21. DOI: https://doi.org/10.1007/s10584-021-03163-4.

[114] IRENA. *Renewable Power Generation Costs in 2019*. Abu Dhabi, 2020.

[115] D. Lugo-Laguna, A. Arcos-Vargas, and F. Nuñez-Hernandez. ``A European Assessment of the Solar Energy Cost: Key Factors and Optimal Technology''. In: *Sustainability* 13.6 (2021). DOI: https://doi.org/10.3390/su13063238.

[116] C. Minke and T. Turek. ``Materials, system designs and modelling approaches in techno-economic assessment of all-vanadium redox flow batteries - A review''. In: *Journal of Power Sources* 376 (2018), pp. 66–81.

[117] J. Noack et al. ``Techno-economic modeling and analysis of redox flow battery systems''. In: *Energies* 9.8 (2016), p. 627.

[118] N. Singh and E. W. McFarland. ``Levelized cost of energy and sensitivity analysis for the hydrogen–bromine flow battery''. In: *Journal of Power Sources* 288 (2015), pp. 187–198. ISSN: 0378-7753. DOI: https://doi.org/10.1016/j.jpowsour.2015.04.114.

[119] H. Xin. ``inc Bromine Flow Battery for PV-Battery Microgrid System Utilization: Analysis, Modeling, Performance, and Field Demonstration''. PhD thesis. University of California Riverside, June 2021.

[120] A. Larsson. *Evaluation of flow battery technology: An assessment of technical and economic feasibility*. 2009.

[121] C. Noack et al. ``Studie über die Planung einer Demonstrationsanlage zur Wasserstoff-Kraftstoffgewinnung durch Elektrolyse mit Zwischenspeicherung in Salzkavernen unter Druck''. In: (2015).

[122] Energy.gov. *Hydrogen and Fuel Cell Technologies Office Multi-Year Research, Development, and Demonstration Plan*. 2016. URL: https://www.energy.gov/sites/default/files/2017/05/f34/fcto_myrdd_fuel_cells.pdf.

[123] T. Ramsden, B. Kroposki, and J. Levene. ``Opportunities for hydrogen-based energy storage for electric utilities''. In: *Proceedings of the NHA annual hydrogen conference. Sacramento*. 2008.

[124] B. D. James et al. *hydrogen storage system cost analysis*. Tech. rep. Strategic Analysis Inc., Arlington, VA (United States), 2016.

[125] T. R. Genevieve Saur. *Wind Electrolysis: Hydrogen Cost Optimization*. 2011. URL: https://www.nrel.gov/docs/fy11osti/50408.pdf.

[126] Eurostat. *Electricity price statistics*. 2021. URL: https://ec.europa.eu/eurostat/statistics-explained/index.php?title=Electricity_price_statistics#Electricity_prices_for_household_consumers.

[127] E. Panos and M. Densing. ``The future developments of the electricity prices in view of the implementation of the Paris Agreements: Will the current trends prevail, or a reversal is ahead?'' In: *Energy Economics* 84 (2019), p. 104476.

[128] C. Perez-Linkenheil. ``EU Energy Outlook 2050 – how will Europe evolve over the next 30 years?'' In: *Energy Brainpool* (2019). URL: https://blog.energybrainpool.com/en/eu-energy-outlook-2050-how-will-europe-evolve-over-the-next-30-years-2/.

[129] D. J. Swider et al. ``Conditions and costs for renewables electricity grid connection: Examples in Europe''. In: *Renewable energy* 33.8 (2008), pp. 1832–1842.